Total Synthesis of Biologically Active Natural Product Employing Catalytic Asymmetric Dearomatization

M.Sc. Thesis

by

Raghunath Polai

Roll no. 2203131026

DEPARTMENT OF CHEMISTRY

INDIAN INSTITUTE OF TECHNOLOGY INDORE

MAY 2024

Total Synthesis of Biologically Active Natural Product Employing Catalytic Asymmetric Dearomatization

A Thesis

Submitted in partial fulfillment of the

Requirement for the award of the degree

of

Master of Science

by

Raghunath Polai

Roll no. 2203131026

INDIAN INSTITUTE OF TECHNOLOGY INDORE

CANDIDATE'S DECLARATION

I hereby certify that the work being presented in the thesis entitled **Total Synthesis of Biologically Active Natural Products Employing Catalytic Asymmetric Dearomatization,** in the partial fulfillment of the requirements for the award of the degree of **MASTER of SCIENCE** and submitted to the **DEPARTMENT of CHEMISTRY, Indian Institute of Technology Indore**, is an authentic record of my work carried out during the period July 2023 to May 2024 under the supervision of **Dr. Debayan Sarkar** (Associate Professor) Department of Chemistry, Indian Institute of Technology Indore. The matter presented in this thesis has not been submitted by me for the award of any other degree of this or any other institute.

Raghunath Polai

Signature of the Student **Raghunath Polai**

This is to certify that the above statement by the candidate is correct to the best of my/our knowledge.

Debayan Sarkar

Signature of the M.Sc. Thesis Supervisor **Dr. Debayan Sarkar**

Raghunath Polai successfully gave his M. Sc. oral Examination held on 10/05/2024.

Signature of supervisor of M. Sc. Thesis	Convener, DPGC
Date:	Date:
Signature of PSPC Member	Signature of PSPC Member
Prof. Sampak Samanta	**Dr.** Dipak Kumar Roy
Date:	Date:

Prefatory Notes

Nuclear magnetic resonance spectra

^{1}H and ^{13}C NMR spectra were recorded on a Bruker (500MHz, and 125 MHz, respectively). Chemical shifts are reported in delta (δ, chemical shift relative to deuterochloroform (7.26 ppm) for ^{1}H NMR & 77.0 for ^{13}C NMR). Data for ^{1}H reported as follows- Chemical shift (δ ppm) (multiplicity, coupling constant (Hz), integration). Multiplicity is recorded as follows: s = singlet, d = doublet, t = triplet, q = quartet, m = multiplet, dd = doublet of doublet.

Chromatography

Chromatography was performed using (100-200mesh) silica gel& neutral active aluminium oxide. Analytical TLC was performed with 0.25 mm coated commercial silica gel plates (E. Merck, DC-Kiesel gel 60 F254) and visualized with UV light, iodine, and vanillin stain. ^{1}H and ^{13}C NMR spectra were recorded on a Bruker (500 MHz and 125 MHz, respectively).

General

All reactions were carried out under oven-dried glassware. All solvents were dried over appropriate desiccant before use. All other reagents were purchased from TCI chemicals, Sigma-Aldrich, and HIMEDIA and used without further purification. Na_2SO_4 was dried in an oven & utilized for drying the crude reaction mixture before chromatography.

ACKNOWLEDGEMENTS

The research described in this report entitled Dual Catalytic **"Total Synthesis of Biologically Natural Products Employing Catalytic Asymmetric Dearomatization"** was carried out in the Department of Chemistry, Indian Institute of Technology Indore, during the period of my research from July 2023 and onwards under the supervision of Dr. Debayan Sarkar.

Firstly, I would like to express my Gratitude and special thanks to my supervisor, **Dr. Debayan Sarkar**, for his sincere guidance, supervision, and advice from the very first day of my research life, as well as for giving me all valuable experiences throughout my research work. Above all, he encouraged and supported my success and failure throughout my research career.

This journey at IIT Indore has been a memorable time in my life. I extend my heartfelt thanks to my PSPC members, Prof. Sampak Samanta, Dr. Dipak Kumar Roy, and all the Department of Chemistry IIT Indore faculty members.

Special thanks to Ph.D. mentor **Biswajit Das**, lab mates and seniors Shantanu Samanta, Sangita Bishi, Bhabani Sankar Lenka, Niladri Sekhar Roy, Priya Ranjan Sahoo, Ramakant Mishra, Argha Dey, Subarna Roy and Nabanita Dey for their kind co-operation and helping nature throughout my research, which created an excellent working environment, which helped me a lot.

During this journey, many people helped and encouraged me in various ways. I express my heartiest thanks to my friends. Thanks to all those colleagues whose names are unwillingly left.

I could only have started my research with the encouragement and inspiration from my parents, beloved brothers and sisters, and relatives. I dedicate this work to them to honor their love and kind support during this research period.

Raghunath Polai
M. Sc. 2nd year
Roll No. 2203131026
Department of Chemistry

Dedicated To
my Parents and
Brothers

ABSTRACT

Using RFTA and TEAI as the catalytic amounts, a very effective and successful peroxidative dearomatized organic transformation was achieved by visible light catalysis. No metal is used in this transition, and no additional additives like buffer are used. Outstanding yields were demonstrated over a wide range of substrate scopes using ortho-selective for naphthol and para-selective for phenol. Reaction Condition is notable and rather straightforward.

TABLE OF CONTENTS

LIST OF FIGURES

LIST OF SCHEMES

ACRONYMS

$CDCl_3$	Chloroform-d
$CHCl_3$	Chloroform
THF	Tetrahydrofuran
DCM	Dichloromethane
DMSO	Dimethyl sulfoxide
TBAB	Tetra Butyl Ammonium bromide
TBAI	Tetra Butyl Ammonium Iodide
TEAB	Tetra Ethyl Ammonium Bromide
TEAI	Tetra Ethyl Ammonium Iodide
HRMS	High-resolution mass spectrometry
TBHP	Tert Butyl Hydroperoxide
Cs_2CO_3	Cesium Carbonate
K_2CO_3	Potassium carbonate
LCMS	Liquid chromatography-mass spectrometry
EtOH	Ethanol
RFTA	Riboflavin Tetraacetate
MeOH	Methanol
MeCN	Acetonitrile
Na_2SO_4	Sodium sulfate
DBU	1,8-Diazobiclo[5.4.0]undecen-7-ene1
NMR	Nuclear magnetic resonance
NH_4Cl	Ammonium chloride
NaN_3	Sodium Azide
LED	Light Emitting Diode
PPh3	Triphenylphosphine
NEt_3	Triethyl amine
EtOAc	Ethyl Acetate
DMF	Dimethyl Formamide
Et_2O	Diethyl Ether
TLC	Thin layer chromatography
UV	Ultra-violet
UV-Vis	Ultra-violet and visible

X	Halide
PTAB	Phenyl Trimethyl Ammonium Tribromide
$NaBH_4$	Sodium Borohydride
NaOH	Sodium Hydroxide
KOH	Potassium Hydroxide
DABCO	1,4-diazabicyclo[2.2.2]octane
TEMPO	2,2,6,6-Tetramethylpiperidin-1-yl)oxyl
TMP	2,2,6,6-Tetramethylpiperidine
$^{13}C\{H\}$	Proton decoupled ^{13}C NMR

NOMENCLATURE

˚C	Degree Celsius
h	hour
Hz	Hertz
M	Molar
mL	Millilitre
mg	Milligrams
MHz	megahertz
mmol	millimole
ppm	Parts per million

Catalytic Approach Towards Oxidative Dearomatization of Arenols

Objective:

The main objective of this project is to dearomatize various substituted phenols and naphthols via a photocatalytic approach and their synthesis to break the molecular complexity.

Chapter-1 (INTRODUCTION)

1.1 General Introduction

Aromatic hydrocarbons are the economic class of feedstock that is available in plenty all around. Generating multi-functional three-dimensional structures from these simple planer aromatic compounds allows fast access to solve complexity at higher levels. The focal point is that this crucial transformation makes a wide range of carbon-carbon and carbon-heteroatom bond formations possible.

The hypervalent iodine reagents are the most employed non-metallic oxidative decorative reagents and catalysts. Willgerodt synthesized the first hypervalent iodine reagents, which are λ^3 and λ^5 types, among which PIDA, Koser's reagent (HTIB), PIFA, and IBX, etc., have been employed rigorously.[1]

Varied attempts were undertaken towards oxidative dearomatization of planar arenes employing asymmetric dearomatization reagents. But till now, there have been less successful economic efforts in designing protocols for sustainable dearomatization. To a broader extent, hyper-valent iodine-based reagents have been utilized to accomplish this elegant transformation, albeit generalizability and scaling up have been issues with these reactions.

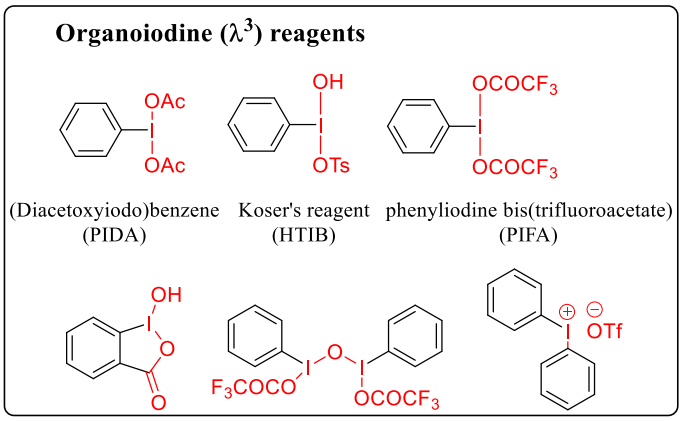

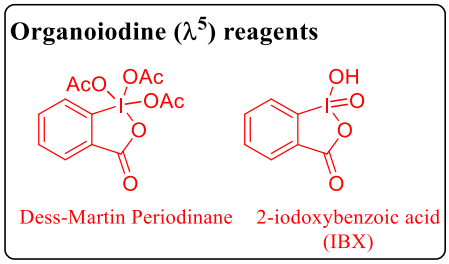

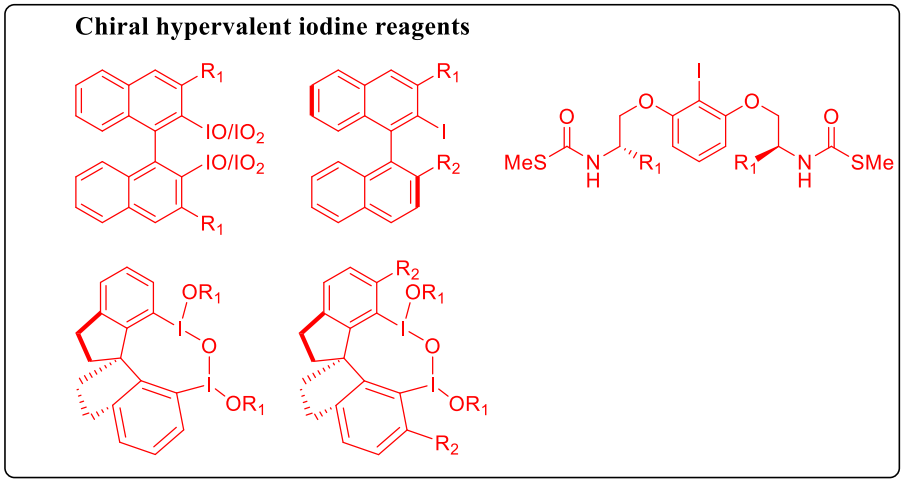

Ligand-assisted asymmetric induction in the dearomatization of phenols and catalytic asymmetric dearomatization reactions (CADRs) have also been prominent in recent years. The following table shows some of the essential iodine-based asymmetric dearomatization reagents.

In particular, the CADRs You. et. al. developed have attracted worldwide attention.[2] Transition metal complexes based on Os, Ru, Re, Cr, Mn, etc. in stoichiometric amounts have shown predominance in these transformations; the toxicity and cost related to the use of these complexes behave as deterrents of their ample use in synthesis.[3,4,5] Apart from the chemical processes, the microbial arene oxidations to the corresponding cis-1,2-dihydrocyclohexadienes can be

considered one of the most potent techniques. However, the required bacterial stains are highly substrate-specific. Thus, biomimetic protocols towards the dearomatization of arenes have remained challenging.

The exhaustive resonance stabilization renders arenes remarkably unreactive as starting materials. Protocols that can circumvent this inertness are still being determined. This inertness often leads to side reactions like dimerization and decomposition of the substrate. A notable contribution from our lab includes the tribromide as a critical resource for dearomatization.[6-9] Our perruthenate-generated catalyzed ipso-decorative spiro-etherification and spiro-amidation of phenols delivers an insight into catalytic decorative spirocyclasitation.[10]

However, we envisioned that the photocatalytic oxidation of phenols with visible light in the presence of aerial oxygen as an oxidant would be a specific advancement of decorative chemistry. With our stepper into new experiment onto these reactions, a recent report from Alison group disclosed the photocatalytic oxidative dearomatization of anisaldehyde derivatives. However, the photocatalytic oxidation was only possible with anisaldehyde derivatives. Limitations are with substrate scope and use of buffer additives.

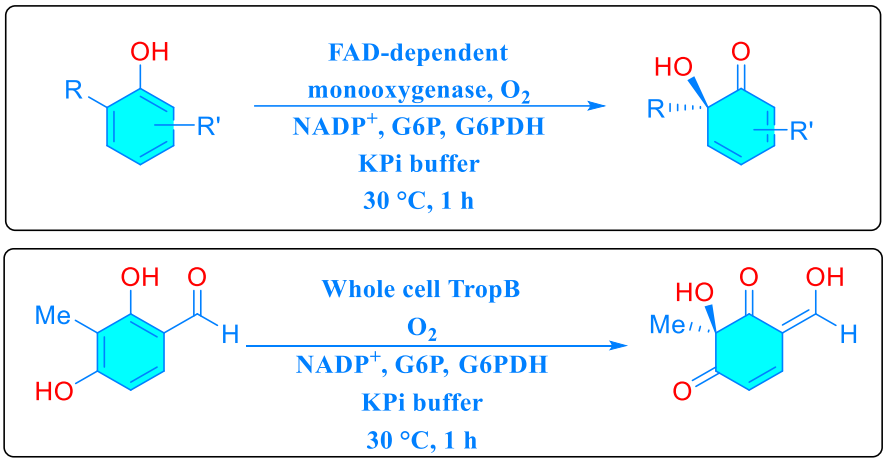

Figure 1. Alison Group Scheme

Although the present approach is an exhaustive enhancement, at this point, we envisioned employing our tribromide/triiodide catalysis into the dearomatization chemistry. Also, the photo-oxidation of bromide or

iodide is noteworthy as it directs towards an essential protocol of converting solar energy to the stirred energy of bromide/iodide. The photo-assisted conversion of bromide to bromine has been coming out under acidic conditions like TiO_2, $NbCl_5$, Fe^{2+} ion, Anthraquinone, Colloidal TiO_2, Rhodium and Chromium complexes, Platinum-Rhodium complexes, Platinised-TiO_2 Powders, albeit this requires a highly energetic UV-radiation—only a recent report by Chang. Et. al. report a visible light conversion of bromide ion to bromine in the presence of $[Ru(deeb)2(dumpy)](PF_6)_2$ and 4-bromobenzene diazonium tetrafluoroborate (ArN_2BF_4).

Thus, with our prolonged experience on tribromide-mediated dearomatization, we envisaged that a dual catalytic mode might be designed that would oxidize the halides to trihalides and, in the course, would also carry out the photocatalytic oxidation of phenols and β-Naphthols. The chances of polymerization or complete decomposition of the cyclohexadiene were relatively high in the HBr/HI environment.

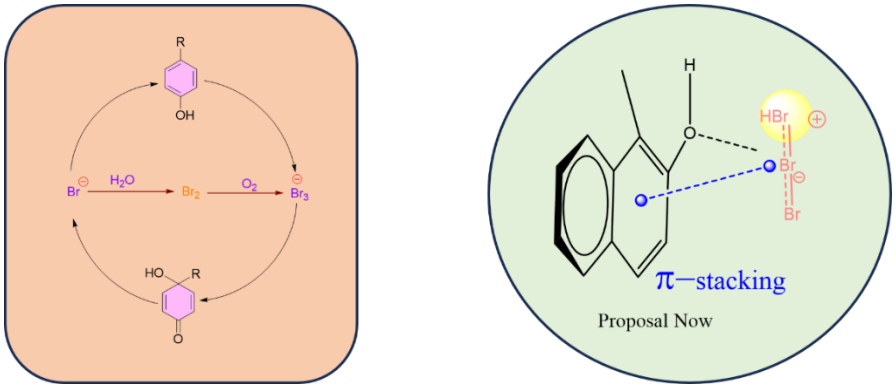

Figure 2. Bromide to tribromide and its π-stacking

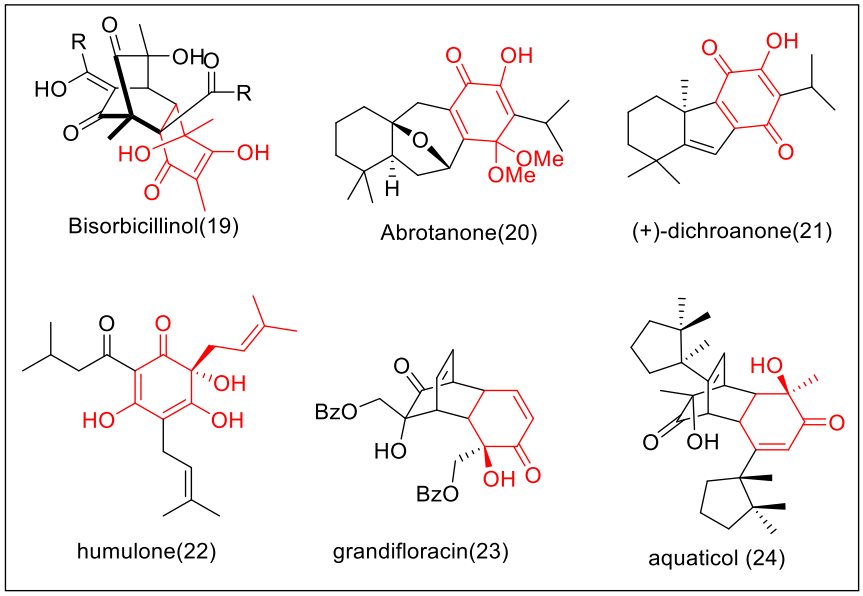

Figure 3. Natural Products having Cyclohexadienones moiety

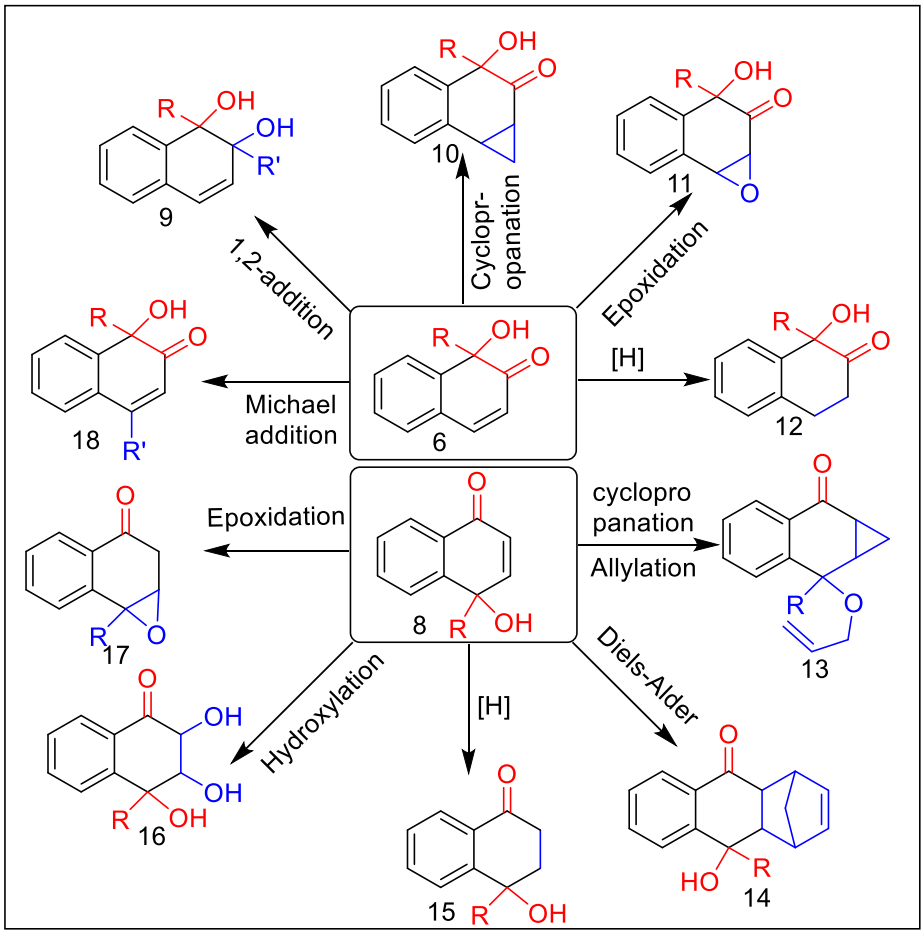

Figure 4. Future Functionalization

1.2. Why Dearomatization?

In synthetic chemistry, dearomatization processes are essential for synthesizing complex compounds. Chemists can introduce new functional groups and produce a variety of structures with distinct features by breaking the aromaticity of a molecule. Reactive sites are frequently absent from aromatic compounds, which reduces their adaptability in chemical reactions. These reactive sites become accessible by dearomatization, allowing for further molecular modification and functionalization. Not only do many natural compounds include aromatic rings, but they also serve various purposes. To effectively synthesize these complicated natural compounds, dearomatization techniques are crucial. Since it makes it possible to modify aromatic medicines to enhance their pharmacological qualities—such as bioavailability, potency, and selectivity—dearomatization is important to medicinal chemistry. Dearomatization reactions can play a crucial role in catalytic processes by facilitating the more efficient and sustainable synthesis of useful intermediates or products. Since aromatic compounds have special features, they are widely used in materials research. Dearomatization can be used to modify these attributes or add aromatic units to more complex molecular structures, creating new materials with customized qualities. In essence, dearomatization broadens the synthetic toolbox, allowing chemists to explore a wider variety of chemical space and create new compounds with different applications spanning from pharmaceuticals to materials science.

There are many hazardous petroleum by-products, such as benzene, phenol, xylene, toluene, styrene, and naphthalene. They can cause severe health issues. It is possible to convert poisonous aromatic petroleum hydrocarbons into less dangerous or more beneficial molecules by using dearomatization techniques. Aromatic compounds undergo structural changes and functional group introduction during deodorization processes, which produce a variety of chemical products. In comparison to the original aromatic hydrocarbons, these molecules may be less harmful as a result of this diversification. Breaking a

molecule's aromaticity, or dearomatization, can increase its reactivity and make it more susceptible to other chemical changes. The molecules that remain after the aromatic feature is eliminated might have altered chemical and biological characteristics, which could lessen their toxicity. Different catalysts can be used to catalyze dearomatization reactions, such as enzymes, transition metals, and organocatalysts. Catalytic dearomatization processes typically work under mild reaction conditions, which minimize energy consumption and waste generation while facilitating the conversion of toxic aromatic hydrocarbons into less hazardous or beneficial products. To detoxify contaminated sites, dearomatization techniques can be used in environmental remediation projects. These techniques work by either transforming toxic aromatic hydrocarbons into less dangerous compounds or by promoting their breakdown into harmless byproducts. All things considered, dearomatization techniques provide a flexible way to alter aromatic petroleum hydrocarbons, possibly lessening their toxicity and increasing their usefulness in various applications, such as chemical synthesis and environmental cleanup.

1.3 Why Visible Light Catalysis?

Compared to other energy sources, visible light is abundant and environmentally favorable. Photocatalysis uses this energy source to perform chemical transformations, lowering dependency on non-renewable resources and generating less waste. Visible light photocatalysis frequently functions at mild reaction conditions, such as room temperature and atmospheric pressure, which can reduce energy consumption and the formation of undesirable byproducts. Photocatalysis provides fine control over reaction pathways and selectivity, enabling the production of complex compounds with great efficiency and specificity. This selectivity is very useful in the production of medicines and specialty compounds. It is compatible with a wide range of functional groups, activating normally inert substrates and promoting the synthesis of complex compounds that would be

difficult to get using traditional methods. Photocatalytic reactions frequently occur with high atom economy, which means that the majority of the starting material is integrated into the final product. This efficiency decreases waste while improving the overall sustainability of chemical operations. It supports various chemical changes, such as C-C and C-X bond formation, hydrogenation, oxidation, and rearrangements. This adaptability makes it an invaluable resource for synthetic chemists in academia and industry. It has applications in drug discovery and development, allowing for the production of new drug candidates and the modification of existing compounds to improve their pharmacological properties. Overall, visible light catalysis provides a sustainable, efficient, and adaptable approach to chemical synthesis, with applications ranging from medicines to materials research and beyond. Its value grows as researchers investigate new photocatalytic processes and broaden the range of its uses.

Chapter-2 (Experimental Section)

Present Work

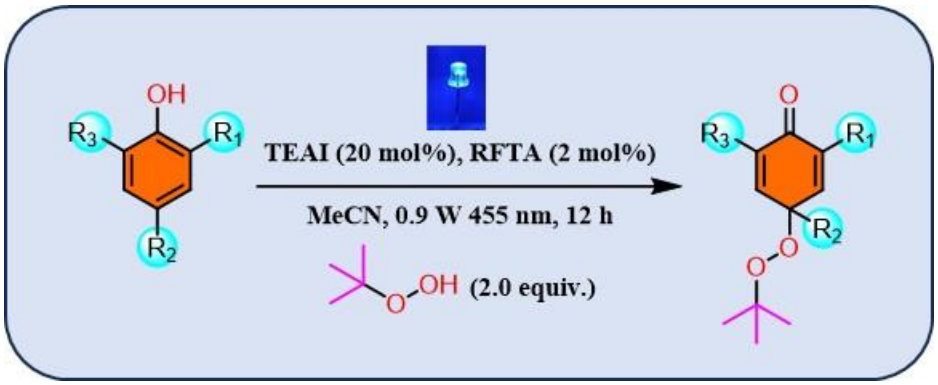

Scheme1. 1a

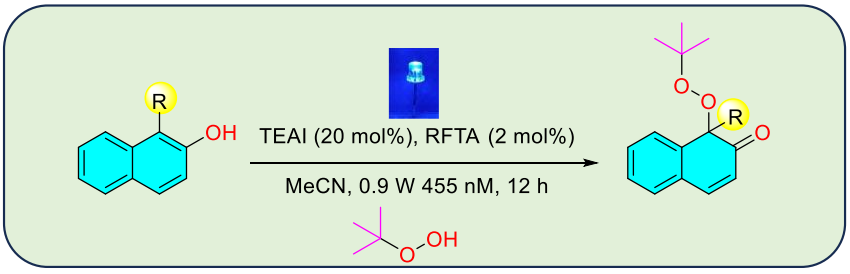

Scheme 1. 2a

Condition Optimization:

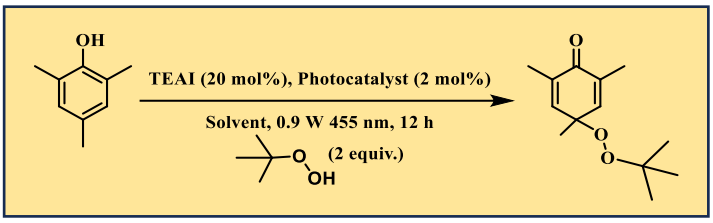

Different Photocatalyst and Solvents were screened:

Entry No.	Photosensitiser (2 mol%)	Solvent	Time (h)	Yield[a] (%)
1	4CzIPN	MeCN : H_2O = 10 : 1	12	65
2	Eosin-blue	MeCN : H_2O = 10 : 1	12	49
3	g-C_3N_4	MeCN : H_2O = 10 : 1	12	62
4	9-Mesityl-10-methylacridinium perchlorate	MeCN : H_2O = 10 : 1	12	75
5	Without RFTA	MeCN : H_2O = 10 : 1	12	Trace
6	RFTA	MeCN : H_2O = 10 : 1	12	74
7	RFTA	Dry Toluene	12	72
8	RFTA	Dry MeCN	12	73
9	Rose Bengal	MeCN : H_2O = 10:1	12	56
10	Eosin-Y	MeCN : H_2O = 10:1	12	52
11	RFTA	MeCN	12	76

Table. 1 Optimization of photosensitizer and solvent.

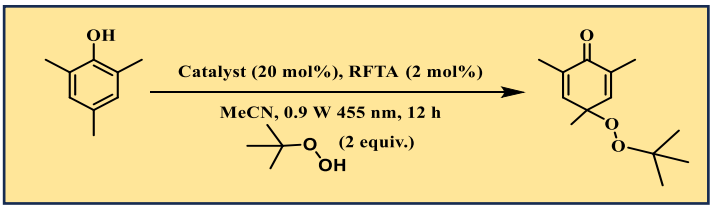

Catalyst (20 mol%)	Yield (%)
TBAI	67
TBAB	70
TEAI	76

Substrate Scopes for Scheme 1.1a:

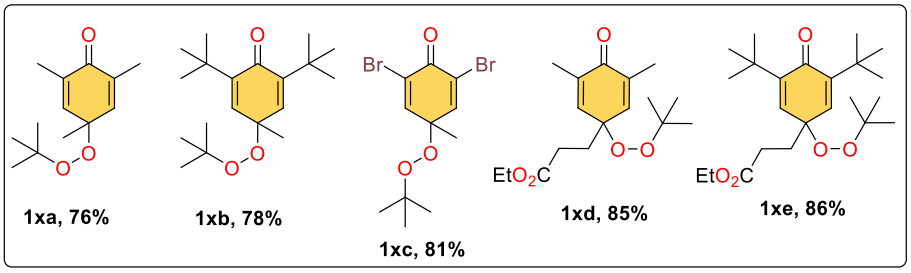

Figure 5. Substrate Scopes of Scheme 1.1a

Substrate Scopes for Scheme 1.2a:

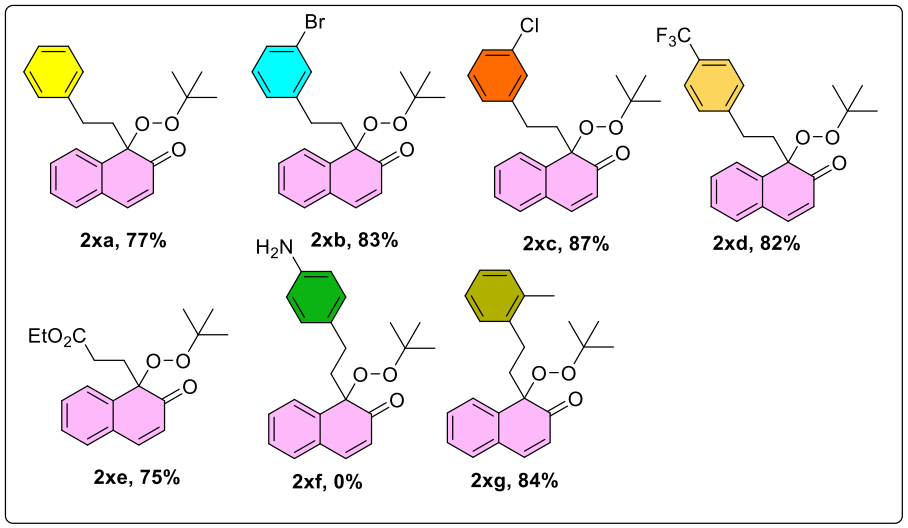

Figure 6. Substrate Scopes of Scheme 1.2a

2.1 General Experimental Procedure for Scheme 1.1a and 1.2a:

In a glass vial, substituted phenols or naphthols were dissolved in MeCN, followed by tetra ethyl ammonium iodide (20 mol%), Riboflavin tetraacetate (2 mol%), and tertbutyl hydroperoxide (2.0 equiv.). Following the septum closure of the glass vial, the reaction vial

was irradiated with a 0.9 w 455 nm LED under stirring in a specially designed cooling system at 25 °C. LED visible through the bottom glass (0.5 cm to LED). The reaction mixture was concentrated at reduced pressure and subjected to column chromatography (neutral alumina).

Plausible Mechanism:

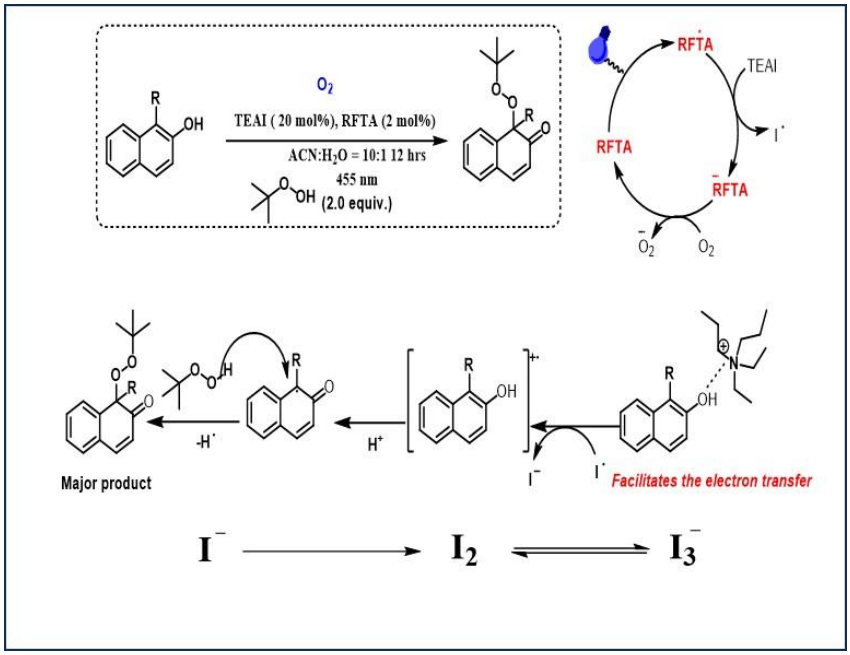

2.2 General experimental procedure for the synthesis of phosphonium salts:

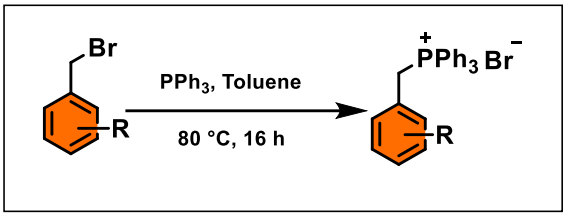

scheme 1. 3a

To a well-stirred solution of triphenylphosphine and toluene, substituted benzyl bromide was added and stirred for 16 h at 80 °C. The white solid was filtered off after reaching the reaction mixture at room temperature.

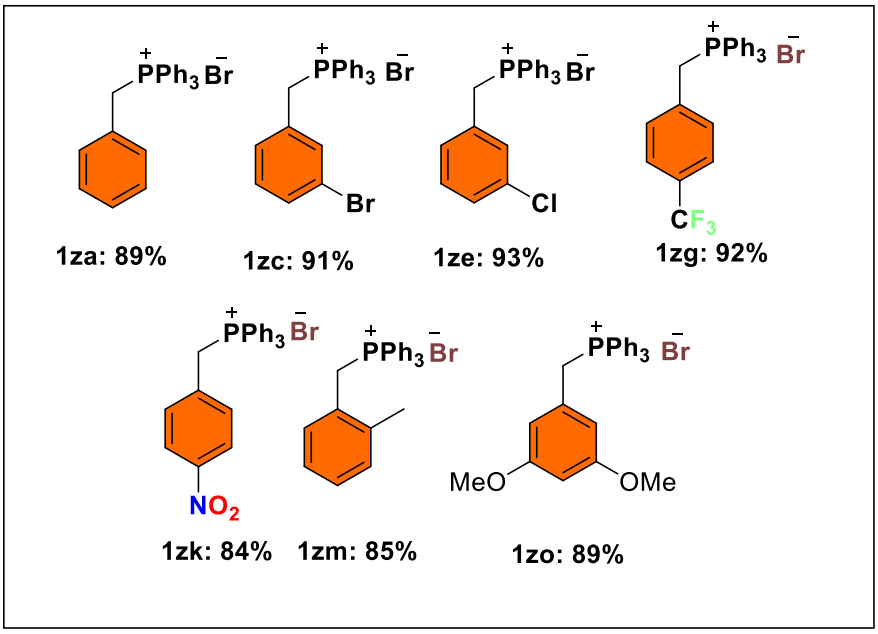

Compound 1za, 1zc, 1zk, 1ze, 1zg, 1zk, 1zm, and 1zo were synthesized following the reported procedure with 89%, 91%, 93%, 92%, 84%, 85% and 89% yield respectively.

2.3 General experimental procedure for Wittig reaction:

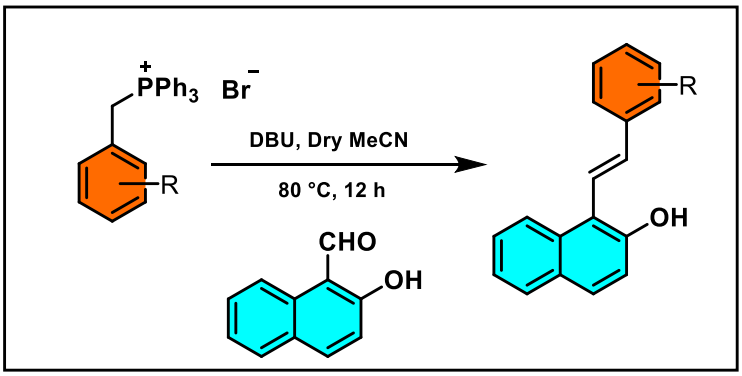

scheme 1. 4a

DBU (6.684 mmol) was added to a well-stirred solution of benzyltriphenylphosphonium bromide (5.57 mmol), 2-hydroxy-1-naphthaldehyde (4.64 mmol) and dry MeCN (40 ml). After refluxing for 12 h, The reaction mixture was concentrated at reduced pressure. column chromatography was performed to obtain the crude product on 100-200 mesh silica gel (Hexane/EtOAc).

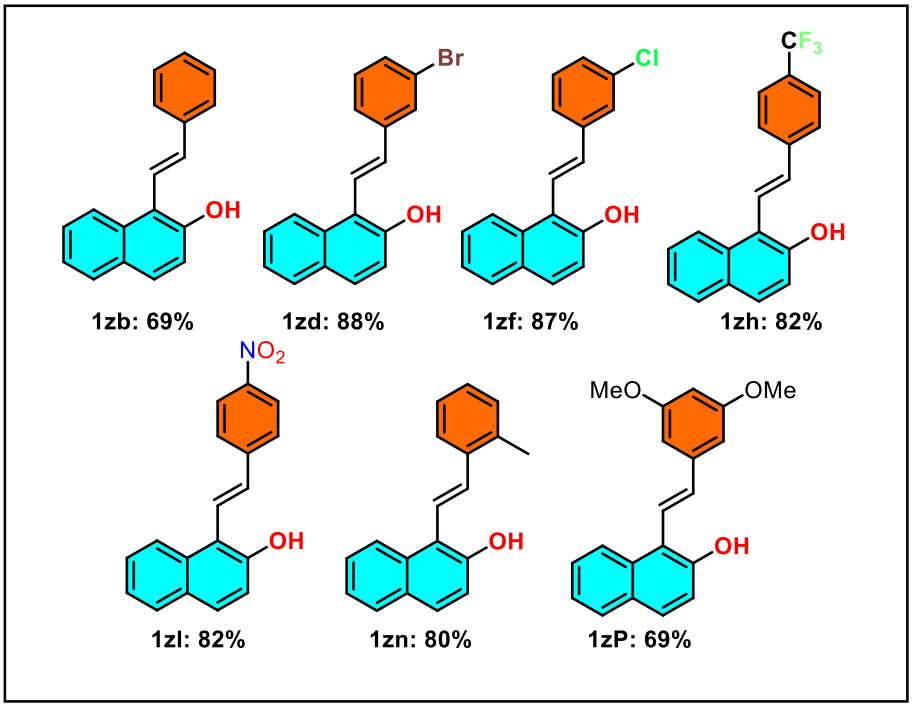

Compound 1zb, 1zd, 1zf, 1zh, 1zl, 1zn and 1zp were prepared by following the reported procedure with 69%, 88%, 87%, 82%, 82%, 80%, and 89% respectively.

2.4 General experimental procedure for Hydrogenation:

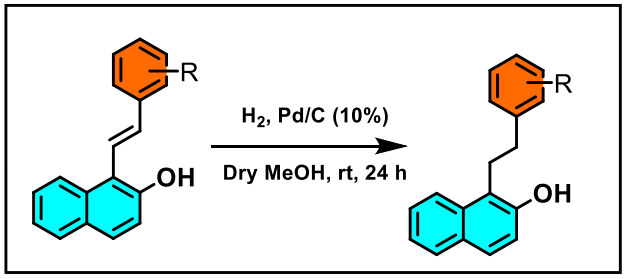

scheme 1. 5a

The compound was dissolved in dry MeOH, and a catalytic amount of 10% Pd/C was added. After being stirred under a hydrogen atmosphere at room temperature for 24 h, the reaction mixture was filtered and concentrated over reduced pressure. The crude mixture was subjected to column chromatography on silica gel (100-200 mesh) (Hexane/EtOAc) to obtain the desired product.

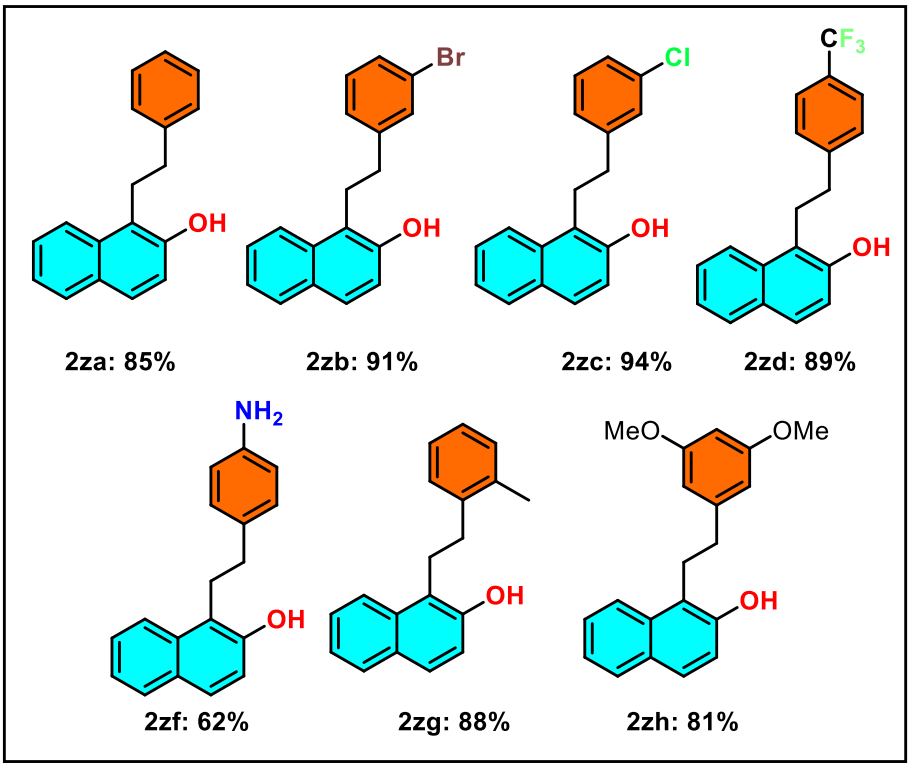

Compound 2za, 2zb, 2zc, 2zd, 2zf, 2zg and 2zh were synthesized by following the reported procedure 85%, 91%, 94%, 89%, 62%, 80% and 81%Yield respectively.

Synthesis of Phenol derivatives:

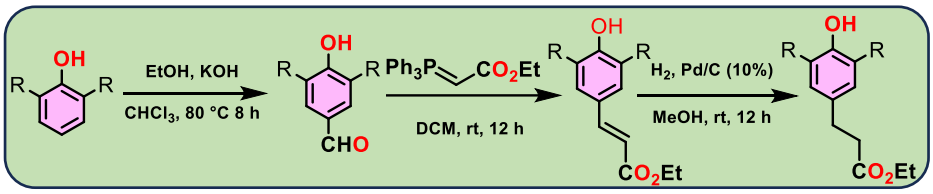

scheme 1. 5a

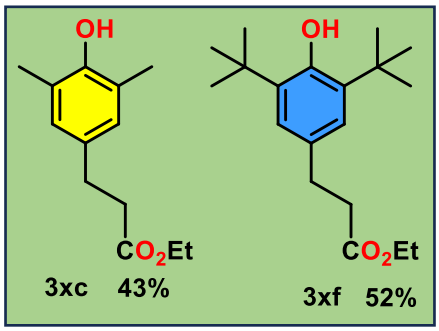

CHAPTER 3: (Results and Discussions)

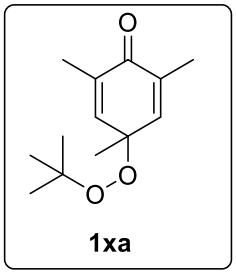

1xa

^{1}H NMR (500 MHz, $CDCl_3$) δ = 6.63 (s, 2H), 1.89 (s, 6H), 1.34 (s, 3H), 1.19 (s, 9H); **^{13}C{^{1}H} NMR** (125 MHz, $CDCl_3$) δ = 187.2, 146.0, 135.1, 26.6, 23.6, 16.1.

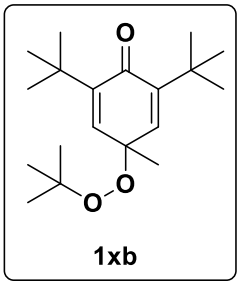

1xb

^{1}H NMR (500 MHz, $CDCl_3$) δ = 6.56 (s, 2H), 2.17 (s, 3H), 1.43 (s, 9H), 1.23 (d, *J* = 1.9 Hz, 18H). **^{13}C{^{1}H} NMR** (125 MHz, $CDCl_3$) δ= 186.8, 146.8, 141.9, 79.5,76.3 34.8, 30.5, 29.6, 26.6.

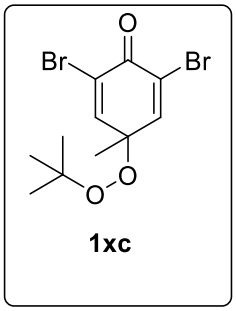

1xc

^{1}H NMR (500 MHz, $CDCl_3$) δ 7.32 (s, 2H), 1.45 (s, 3H), 1.20 (s, 9H). **^{13}C{^{1}H} NMR** (125 MHz, $CDCl_3$) δ 172.65, 151.9, 121.9, 81.0, 80.0, 29.8, 26.4, 22.7.

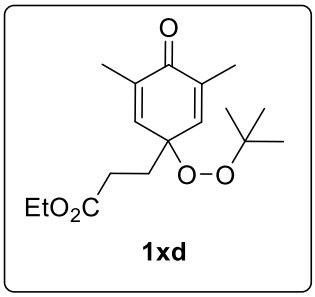

1xd

^{1}H NMR (500 MHz, $CDCl_3$) δ= 6.57 (s, 2H), 4.08 (q, *J* = 7.1 Hz, 2H), 2.22 (t, *J* = 7.9 Hz, 2H), 2.02 (t, *J* = 7.9 Hz, 2H), 1.89 (s, 6H), 1.22 (t, *J* = 7.2 Hz, 3H), 1.18 (s, 9H). **^{13}C{^{1}H} NMR** (125 MHz, $CDCl_3$) δ 187.03, 172.76, 144.16, 136.71, 80.11, 78.43, 60.79, 31.54, 28.91, 26.55, 16.09, 14.29

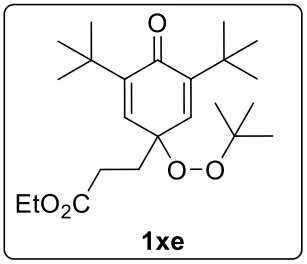

1xe

^{1}H NMR (500 MHz, $CDCl_3$) δ 6.49 (s, 2H), 4.09 (q, *J* = 7.2 Hz, 2H), 2.17 (t, *J* = 8.0 Hz, 2H), 2.01 (t, *J* = 8.0 Hz, 2H), 1.21 (d, *J* = 6.6 Hz, 21H), 1.17 (s, 9H). **^{13}C{^{1}H} NMR** (125 MHz, $CDCl_3$) δ= 186.7, 172.8, 148.4, 140.1, 79.7, 78.4, 60.8, 35.0, 31.9, 29.6, 28.8, 26.6, 14.3.

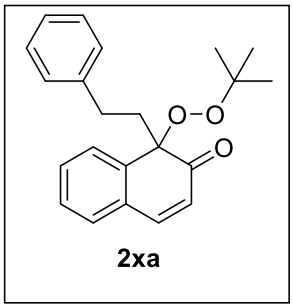

2xa

^{1}H NMR (500 MHz, $CDCl_3$) δ= 7.66 (d, *J* = 7.6 Hz, 1H), 7.46 (td, *J* = 7.5, 1.6 Hz, 1H), 7.39 (d, *J* = 9.9 Hz, 1H), 7.37 – 7.31 (m, 2H), 7.18 (dd, *J* = 8.1, 6.6 Hz, 2H), 7.14 – 7.09 (m, 1H), 6.98 (d, *J* = 7.5 Hz, 2H), 6.21 (d, *J* = 9.9 Hz, 1H), 2.47 (td, *J* = 13.5, 12.6, 3.8 Hz, 1H), 2.33 – 2.20 (m, 2H), 2.05 – 1.98 (m, 1H), 1.16 (s, 9H).**^{13}C{^{1}H} NMR** (125 MHz, $CDCl_3$)

δ= 199.4, 144.9, 143.3, 141.0, 131.2, 130.0, 129.2, 128.5, 128.4, 128.1, 127.4, 126.1, 126.0, 85.1, 80.2, 42.4, 28.9, 26.7

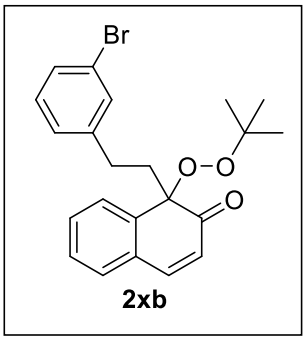

2xb

^{1}H NMR (500 MHz, $CDCl_3$) δ =7.81 (d, *J* = 7.8 Hz, 1H), 7.59 (t, *J* = 7.5 Hz, 1H), 7.55 – 7.42 (m, 3H), 7.28 (dt, *J* = 35.2, 7.2 Hz, 3H), 7.12 (d, *J* = 7.4 Hz, 2H), 6.35 (d, *J* = 10.1 Hz, 1H), 2.61 (dt, *J* = 13.7, 6.2 Hz, 1H), 2.49 – 2.33 (m, 2H), 2.16 (td, *J* = 12.4, 11.3, 3.4 Hz, 1H), 1.31 (s, 9H). **^{13}C{^{1}H} NMR** (125 MHz, $CDCl_3$) δ =199.3, 144.8, 143.1, 140.9, 131.1, 129.9, 129.1, 128.3, 128.2, 128.0, 127.3, 126.0, 125.9, 85.1, 80.1, 42.3, 28.8, 26.6.

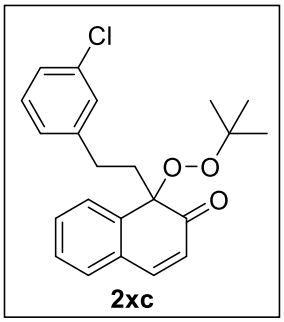

2xc

^{1}H NMR (500 MHz, $CDCl_3$) δ 7.65 (dd, *J* = 7.9, 1.2 Hz, 1H), 7.46 (td, *J* = 7.5, 1.5 Hz, 1H), 7.39 (d, *J* = 9.9 Hz, 1H), 7.37 – 7.30 (m, 2H), 7.13 – 7.07 (m, 2H), 6.97 (d, *J* = 2.2 Hz, 1H), 6.88 (dt, *J* = 6.6, 2.0 Hz, 1H), 6.20 (d, *J* = 9.9 Hz, 1H), 2.51 – 2.42 (m, 1H), 2.31 – 2.19 (m, 2H), 2.04 – 1.97 (m, 1H), 1.16 (s, 9H). **^{13}C{^{1}H} NMR** (125 MHz, $CDCl_3$) δ= 199.1, 144.9, 142.9, 134.0, 1301, 129.5, 129.6, 129.1, 128.4, 128.1, 127.3, 126.5, 126.2, 125.8, 84.8, 80.2, 41.9, 28.1, 26.6.

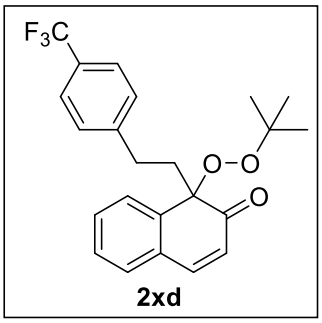

2xd

^{1}H NMR (500 MHz, $CDCl_3$) δ= 7.65 (dd, *J* = 7.8, 1.2 Hz, 1H), 7.48 – 7.42 (m, 3H), 7.40 (d, *J* = 9.9 Hz, 1H), 7.38 – 7.31 (m, 2H), 7.10 (d, *J* = 8.0 Hz, 2H), 6.21 (d, *J* = 9.9 Hz, 1H), 2.58 – 2.49 (m, 1H), 2.36 – 2.26 (m, 2H), 2.06 – 1.99 (m, 1H), 1.15 (s, 9H). **^{13}C{^{1}H} NMR** (125 MHz, $CDCl_3$) δ= 199.1, 145.0, 143.0, 131.1, 130.1, 129.3, 128.7, 128.3, 127.4, 125.9, 125.4, 125.4, 125.3, 125.3, 84.9, 80.4, 41.8, 28.8, 26.7. **^{19}F{^{1}H} NMR** (471 MHz, $CDCl_3$) δ= -62.40.

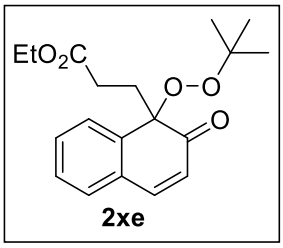

2xe

^{1}H NMR (500 MHz, $CDCl_3$) δ= 7.62 (d, *J* = 7.7 Hz, 1H), 7.42 (t, *J* = 7.5 Hz, 1H), 7.38 – 7.27 (m, 3H), 6.14 (d, *J* = 9.8 Hz, 1H), 4.01 (q, *J* = 7.1 Hz, 2H), 2.30 – 2.18 (m, 2H), 2.15 – 2.04 (m, 2H), 1.17 (d, *J* = 6.4 Hz, 12H). **^{13}C{^{1}H} NMR** (125 MHz, $CDCl_3$) δ=198.7, 172.4, 144.7, 142.7, 130.7, 129.9, 129.1, 128.1, 127.3, 125.5, 84.4, 80.3, 60.5, 35.24, 27.5, 26.5, 14.1

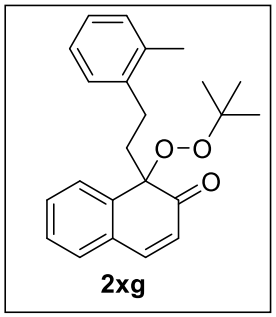

2xg

^{1}H NMR (500 MHz, $CDCl_3$) δ =7.71 (d, *J* = 7.7 Hz, 1H), 7.48 (td, *J* = 7.5, 1.6 Hz, 1H), 7.42 (d, *J* = 10.0 Hz, 1H), 7.39 – 7.32 (m, 2H), 7.05 (d, *J* = 2.7 Hz, 3H), 6.93 (td, *J* = 4.4, 2.3 Hz, 1H), 6.26 (d, *J* = 9.9 Hz, 1H), 2.50 – 2.44 (m, 1H), 2.28 – 2.20 (m, 2H), 2.08 (s, 3H), 1.98 – 1.91 (m, 1H), 1.21 (s, 9H). **^{13}C{^{1}H} NMR** (125 MHz, $CDCl_3$) δ= 199.2, 144.9, 143.2, 139.1, 135.8, 131.1, 130.2, 129.9, 129.1, 128.8, 128.1, 127.3, 126.3, 126.0, 126.0, 85.1, 80.2, 41.5, 26.7, 26.3, 18.9

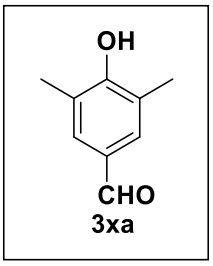

3xa

^{1}H NMR (500 MHz, $CDCl_3$) δ= 9.77 (s, 1H), 7.53 (s, 2H), 6.42 (s, 1H) 2.31 (s, 6H). **^{13}C{^{1}H} NMR** (125 MHz, $CDCl_3$) δ= 192.0, 158.8, 131.2, 129.1, 124.2, 16.0.

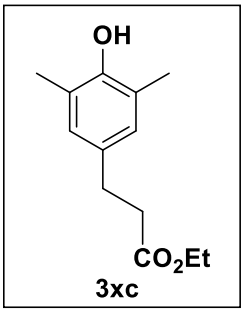

3xc

^{1}H NMR (500 MHz, $CDCl_3$) δ= 7.71 (d, *J* = 15.9 Hz, 1H), 6.44 – 6.38 (m, 2H), 4.38 (q, *J* = 7.1 Hz, 2H), 2.38 (d, *J* = 1.4 Hz, 6H), 1.45 (t, *J* = 7.2 Hz, 3H). **^{13}C{^{1}H} NMR** (125 MHz, $CDCl_3$) δ= 168.0, 155.0, 155.0, 145.3, 128.8, 126.2, 124.1, 124.1, 114.6, 60.4, 16.0, 14.3.

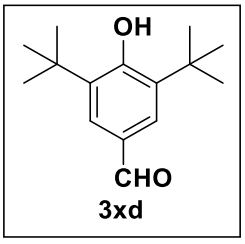

3xd

^{1}H NMR (500 MHz, $CDCl_3$) δ= 9.85 (s, 1H), 7.73 (d, *J* = 7.0 Hz, 2H), 5.85 (s, 1H), 1.51 (d, *J* = 11.9 Hz, 18H). **^{13}C{^{1}H} NMR** (125 MHz, $CDCl_3$) δ= 192.0, 159.8, 136.7, 128.9, 127.8, 34.2, 30.

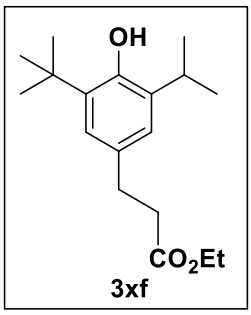

3xf

^{1}H NMR (500 MHz, $CDCl_3$) δ= 7.03 (s, 2H), 5.11 (s, 1H), 4.17 (q, *J* = 7.1 Hz, 2H), 2.93 – 2.88 (m, 2H), 2.65 – 2.61 (m, 2H), 1.47 (s, 18H), 1.28 (t, *J* = 7.1 Hz, 3H). **^{13}C{^{1}H} NMR** (125 MHz, $CDCl_3$) δ= 173.3, 152.2, 136.0, 131.26, 124.9, 60.4, 36.6, 34.4, 31.1, 30.2, 14.4.

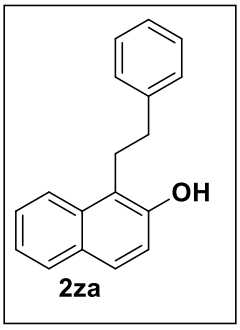

2za

^{1}H NMR (500 MHz, $CDCl_3$) δ= 7.98 (d, *J* = 8.6 Hz, 1H), 7.79 (d, *J* = 8.2 Hz, 1H), 7.63 (d, *J* = 8.8 Hz, 1H), 7.51 (t, *J* = 7.7 Hz, 1H), 7.36 (t, *J* = 7.6 Hz, 1H), 7.33 – 7.21 (m, 5H), 7.00 (d, *J* = 8.8 Hz, 1H), 4.68 (s, 1H), 3.34 (t, *J* = 8.0 Hz, 2H), 2.97 (t, *J* = 7.9 Hz, 2H). **^{13}C{^{1}H} NMR** (126 MHz, $CDCl_3$) δ= 150.7, 142.2, 133.2, 129.6, 128.8, 128.7, 128.6, 128.0, 126.6, 126.3, 123.3, 122.9, 119.5, 118.0, 35.9, 27.7.

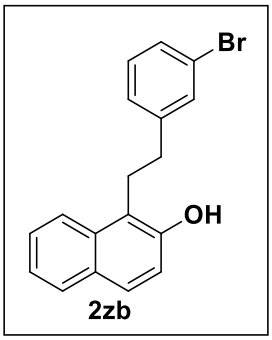

2zb

^{1}H NMR (500 MHz, $CDCl_3$) δ= 7.96 (d, *J* = 8.6 Hz, 1H), 7.76 (d, *J* = 8.1 Hz, 1H), 7.59 (d, *J* = 8.8 Hz, 1H), 7.48 (t, *J* = 7.7 Hz, 1H), 7.35 – 7.19 (m, 6H), 6.95 (d, *J* = 8.9 Hz, 1H), 4.78 (s, 1H), 3.31 (t, *J* = 8.0 Hz, 2H), 2.94 (t, *J* = 8.1 Hz, 2H). **^{13}C{^{1}H} NMR** (125 MHz, $CDCl_3$) δ= 150.7, 142.2, 133.2, 129.6, 128.8, 128.7, 128.6, 128.0, 126.6, 126.3, 123.2, 122.9, 119.6, 118.0, 35.9, 27.6.

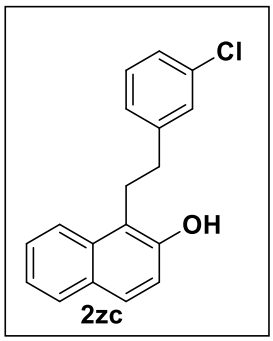

2zc

^{1}H NMR (500 MHz, $CDCl_3$) δ =7.94 – 7.91 (m, 1H), 7.77 (dd, *J* = 8.1, 1.4 Hz, 1H), 7.60 (d, *J* = 8.8 Hz, 1H), 7.50 (ddd, *J* = 8.4, 6.7, 1.4 Hz, 1H), 7.34 (ddd, *J* = 8.0, 6.7, 1.1 Hz, 1H), 7.26 (d, *J* = 2.1 Hz, 1H), 7.20 – 7.15 (m, 2H), 7.09 (dt, *J* = 6.4, 2.0 Hz, 1H), 6.95 (d, *J* = 8.8 Hz, 1H), 4.97 (s, 1H), 3.32 – 3.28 (m, 2H), 2.91 – 2.87 (m, 2H). **^{13}C{^{1}H} NMR** (125 MHz, $CDCl_3$) δ= 150.5, 144.3, 134.3, 133.2, 129.8, 129.6, 128.9, 128.7, 128.2, 126.8, 126.8, 126.4, 123.4, 122.8, 119.4, 117.8, 35.5, 27.2.

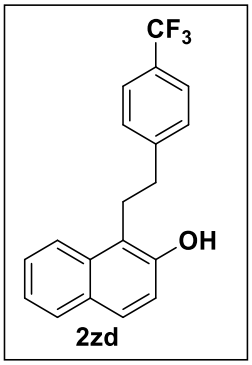

2zd

^{1}H NMR (500 MHz, $CDCl_3$) δ= 7.97 (dd, *J* = 8.4, 1.0 Hz, 1H), 7.83 (dd, *J* = 8.3, 1.4 Hz, 1H), 7.68 (d, *J* = 8.7 Hz, 1H), 7.59 – 7.52 (m, 3H), 7.41 – 7.36 (m, 3H), 7.03 (d, *J* = 8.8 Hz, 1H), 3.41 – 3.36 (m, 2H), 3.06 – 3.01 (m, 2H). **^{13}C{^{1}H} NMR** (125 MHz, $CDCl_3$) δ= 150.6, 146.4, 133.2, 129.6, 128.9, 128.9, 128.2, 126.8, 125.5, 125.4, 125.4, 125.4, 123.3,

122.7, 119.3, 117.8, 35.7, 27.1. **^{19}F{^{1}H} NMR** (471 MHz, $CDCl_3$) δ= -62.14.

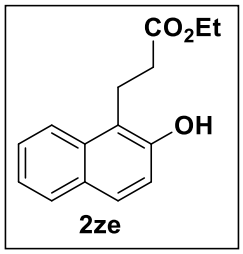

2ze

^{1}H NMR (500 MHz, $CDCl_3$) δ= 8.07 (s, 1H), 7.58 (d, *J* = 5.6 Hz, 2H), 7.47 (d, *J* = 8.9 Hz, 1H), 7.29 (t, *J* = 7.8 Hz, 1H), 7.14 (t, *J* = 7.4 Hz, 1H), 7.01 (d, *J* = 8.9 Hz, 1H), 3.94 (q, *J* = 7.2 Hz, 2H), 3.14 – 3.09 (m, 2H), 2.71 – 2.67 (m, 2H), 1.01 (t, *J* = 7.2 Hz, 3H).

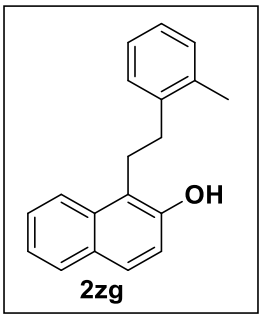

2zg

^{1}H NMR (500 MHz, $CDCl_3$) δ= 8.06 (d, *J* = 8.7 Hz, 1H), 7.85 (d, *J* = 9.8 Hz, 1H), 7.68 (d, *J* = 8.9 Hz, 1H), 7.57 (tt, *J* = 6.9, 1.9 Hz, 1H), 7.41 (ddd, *J* = 8.5, 6.9, 2.2 Hz, 1H), 7.31 – 7.27 (m, 1H), 7.22 (q, *J* = 2.9, 2.4 Hz, 3H), 7.05 (d, *J* = 8.7 Hz, 1H), 4.74 (s, 1H), 3.37 (tt, *J* = 7.4, 2.8 Hz, 2H), 3.06 – 2.99 (m, 2H), 2.37 (d, *J* = 2.6 Hz, 3H). **^{13}C{^{1}H} NMR** (125 MHz, $CDCl_3$) δ= 150.7, 140.4, 136.3, 133.3, 130.5, 129.6, 129.0, 128.8, 128.0, 126.7, 126.5, 126.4, 123.3, 122.8, 119.9, 118.0, 33.2, 26.4, 19.4.

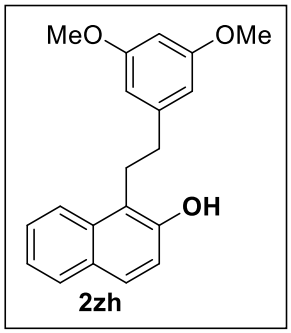

2zh

^{1}H NMR (500 MHz, $CDCl_3$) δ =7.99 (d, *J* = 7.8 Hz, 1H), 7.81 (d, *J* = 6.6 Hz, 1H), 7.65 (d, *J* = 8.7 Hz, 1H), 7.53 (ddd, *J* = 8.4, 6.8, 1.4 Hz, 1H), 7.37 (ddd, *J* = 8.0, 6.8, 1.1 Hz, 1H), 7.04 (d, *J* = 8.8 Hz, 1H), 6.43 (d, *J* = 2.4 Hz, 2H), 6.38 (t, *J* = 2.3 Hz, 1H), 3.77 (s, 6H), 3.39 – 3.34 (m, 2H), 2.96 – 2.91 (m, 2H). **^{13}C{^{1}H} NMR** (125 MHz, $CDCl_3$) δ =161.0, 150.9, 144.6, 133.2, 129.6, 128.1, 128.0, 126.2, 123.2, 122.8, 119.5, 118.0, 106.6, 98.3, 55.4, 36.2, 27.4.

CHAPTER 4: (Characterizations)

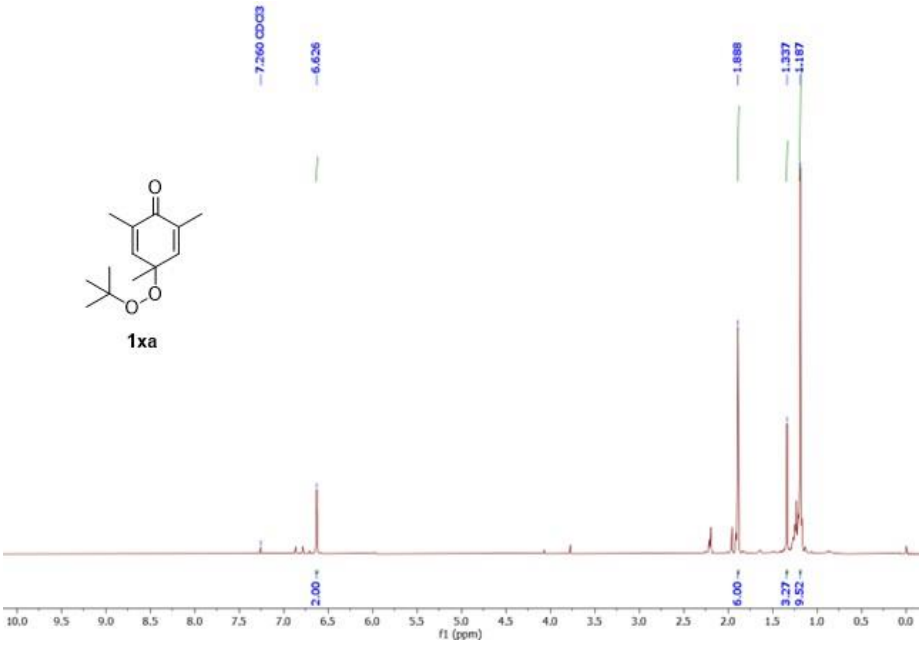

Figure 7. **^{1}H NMR** of Compound **1xa**

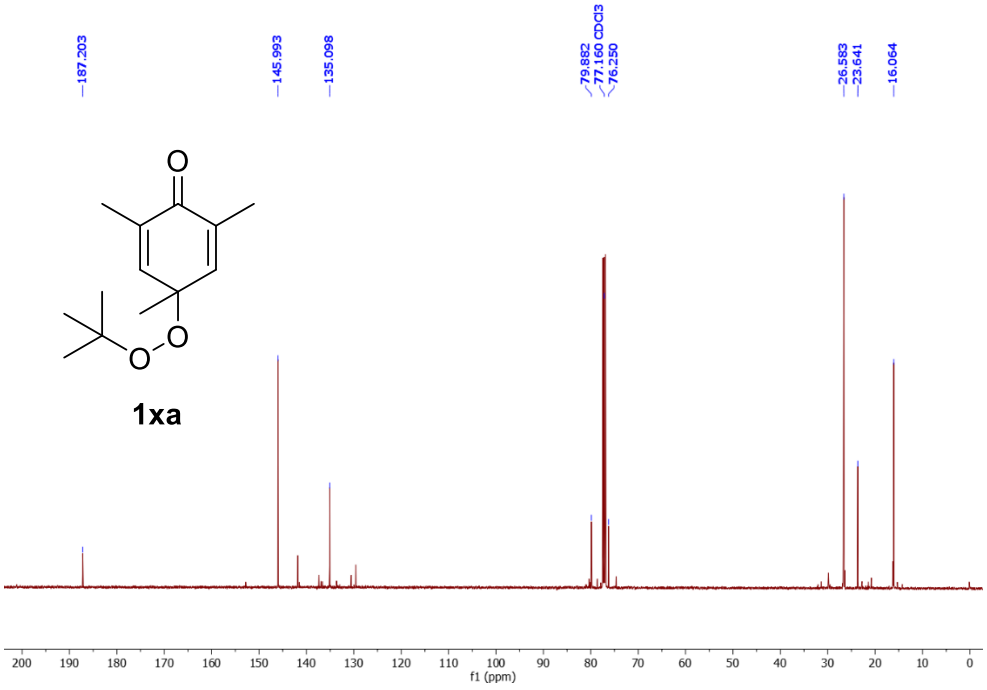

Figure 8. $^{13}C\{^{1}H\}$ NMR of Compound **1xa**

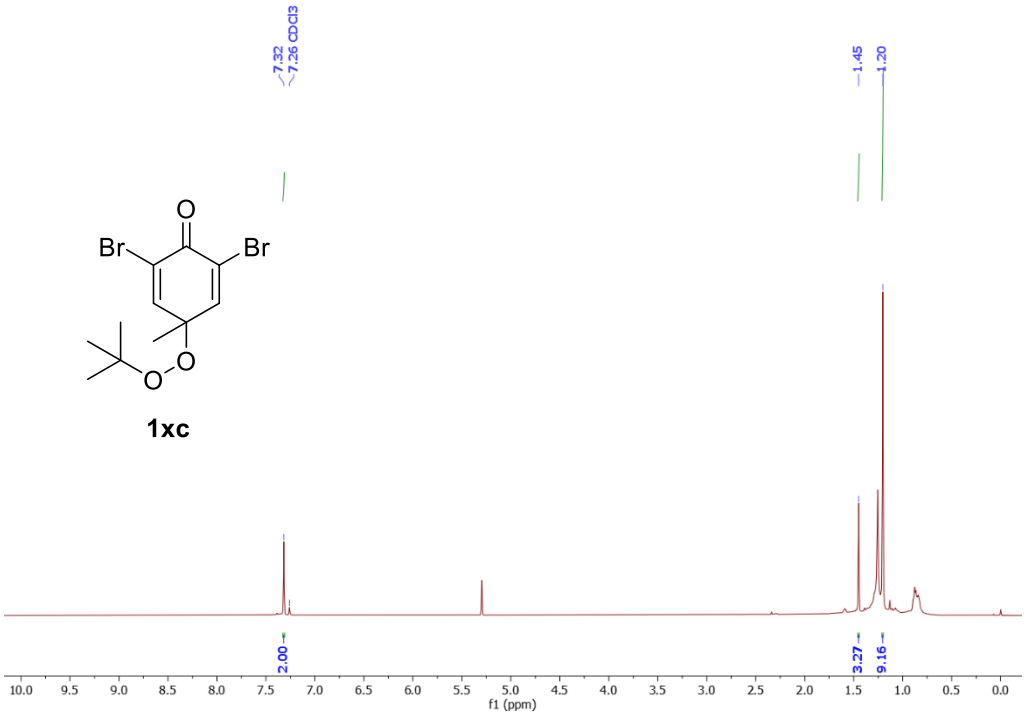

*Figure 9. ^{1}H NMR of Compound **1xc***

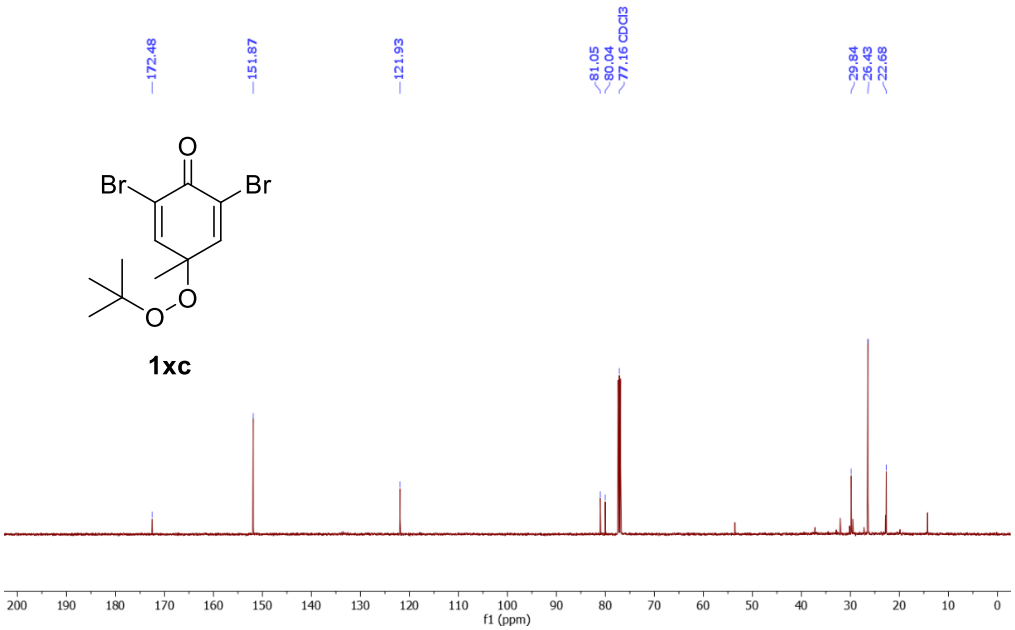

Figure 10. $^{13}C\{^{1}H\}$ **NMR** of Compound **1xc**

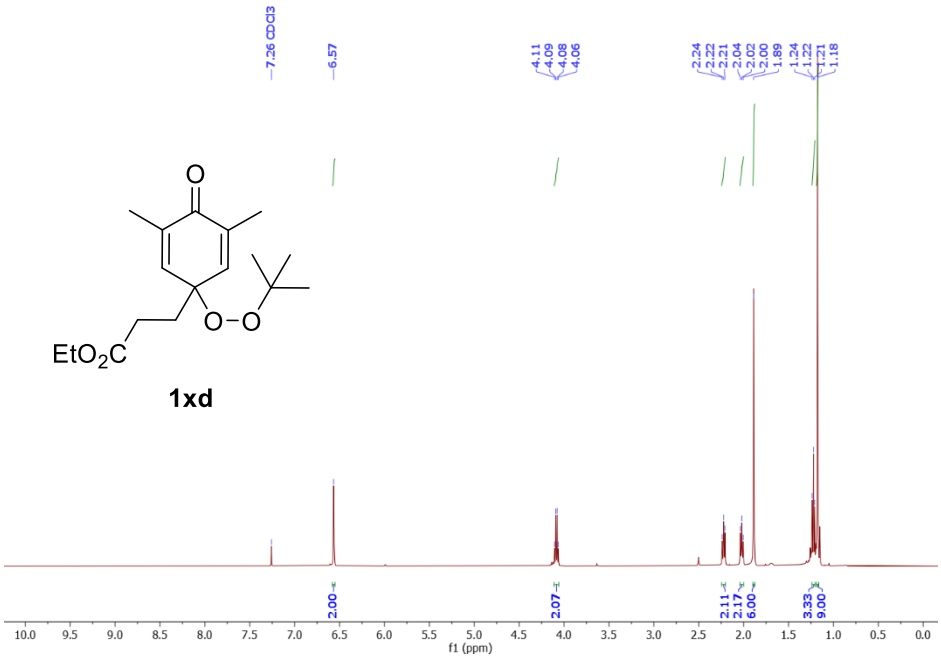

Figure 11.^{1}**H NMR** of Compound **1xd**

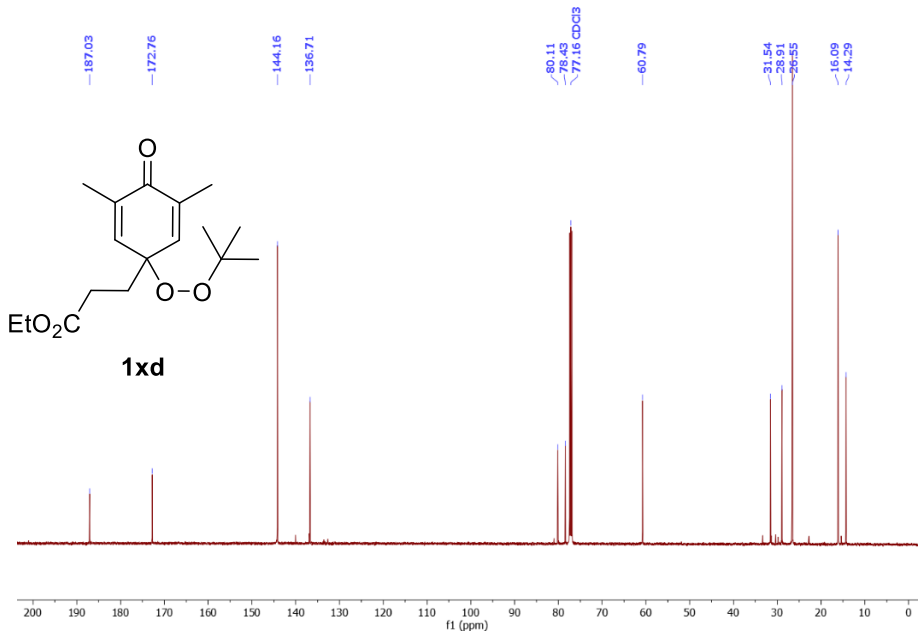

Figure 12. $^{13}C\{^{1}H\}$ **NMR** of Compound **1xd**

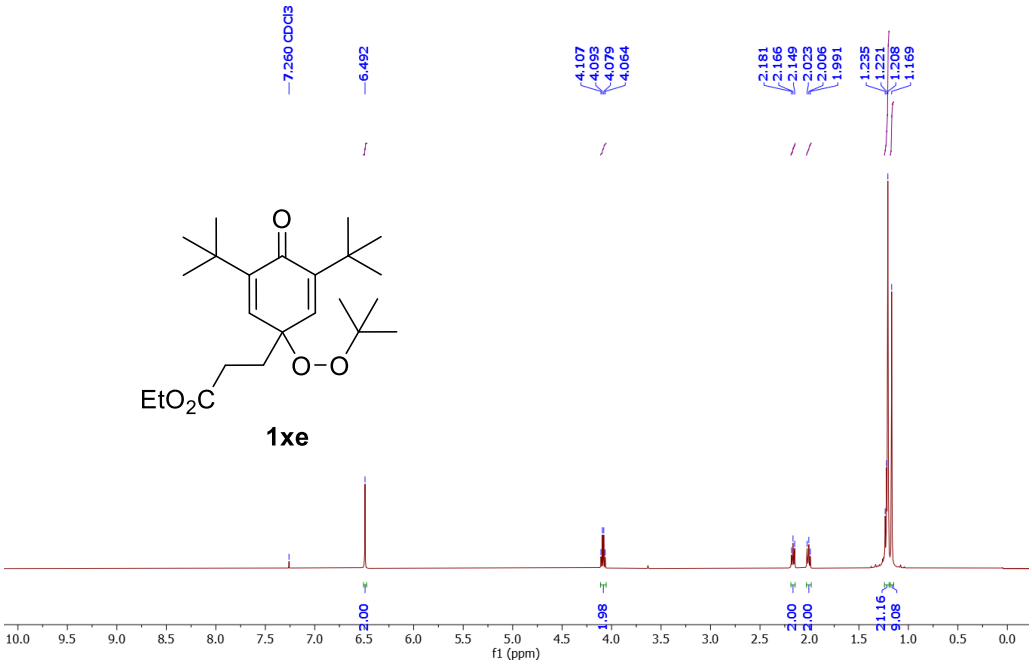

Figure 13. ^{1}H **NMR** of Compound **1xe**

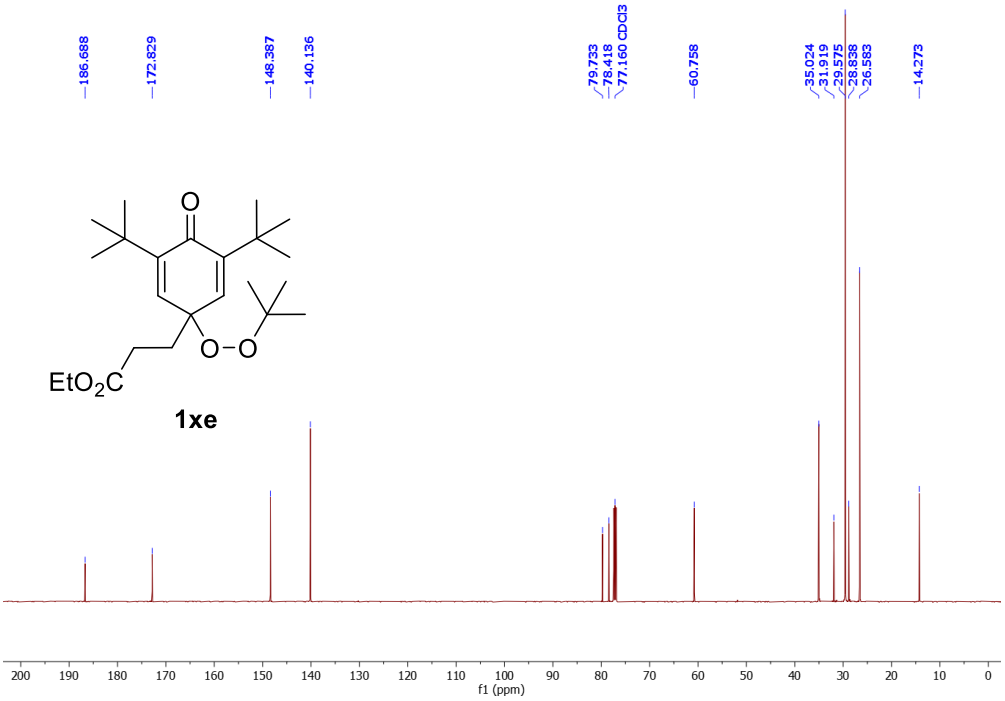

Figure 14. $^{13}C\{^{1}H\}$ **NMR** of Compound **1xe**

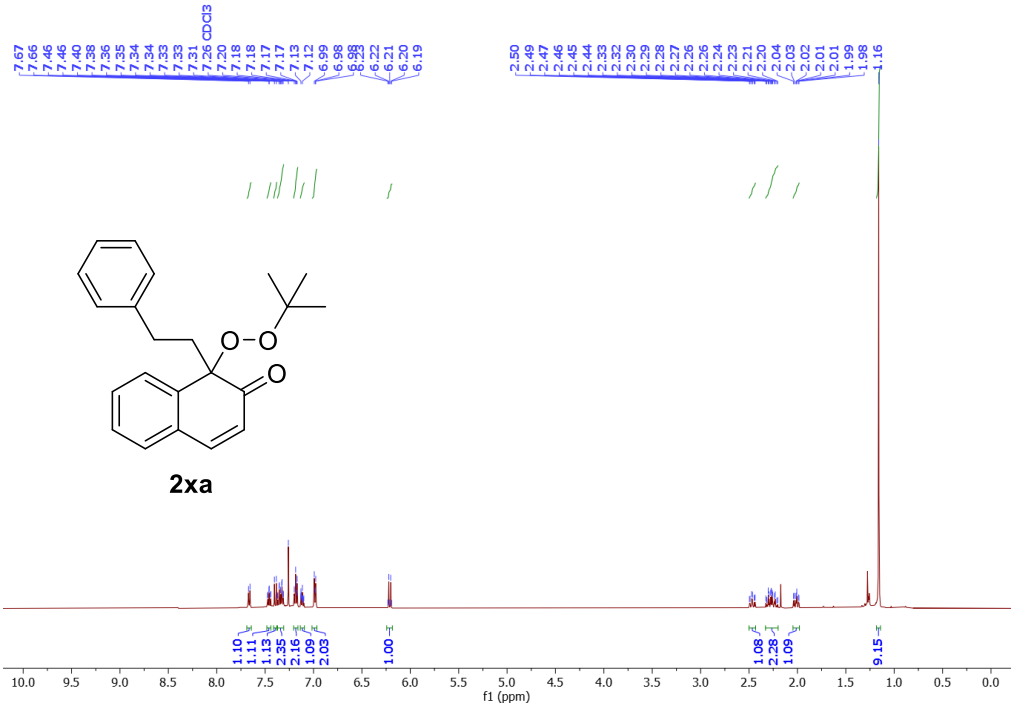

Figure 15. ^{1}H **NMR** of Compound **2xa**

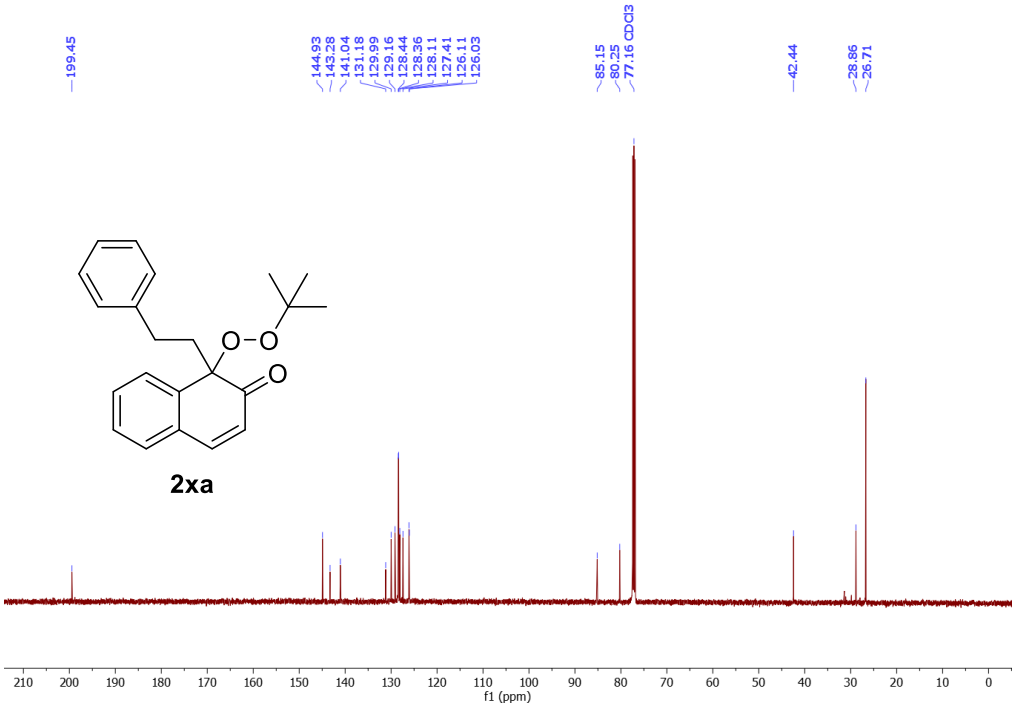

Figure 16. $^{13}C\{^{1}H\}$ **NMR** of Compound **2xa**

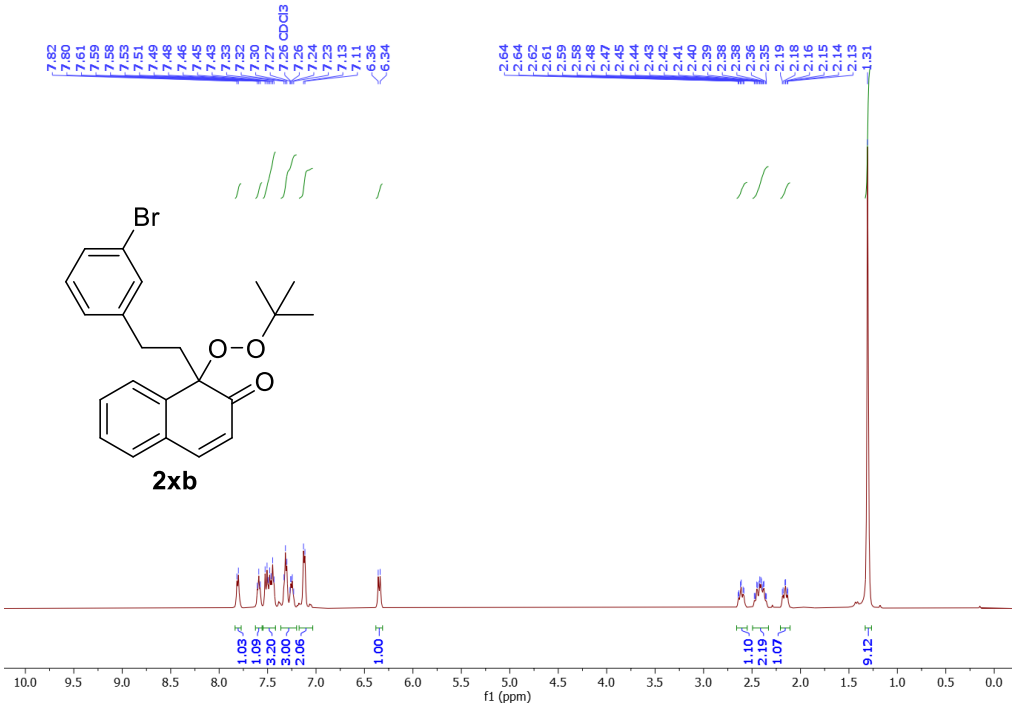

Figure 17. ^{1}H **NMR** of Compound **2xb**

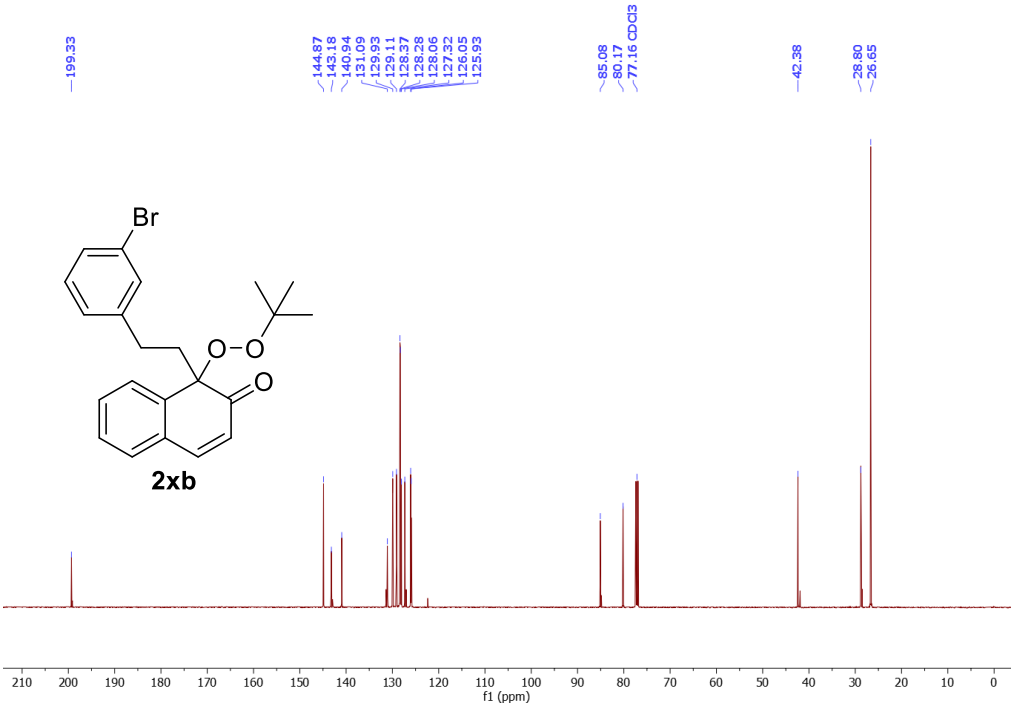

Figure 18. $^{13}C\{^{1}H\}$ **NMR** of Compound **2xb**

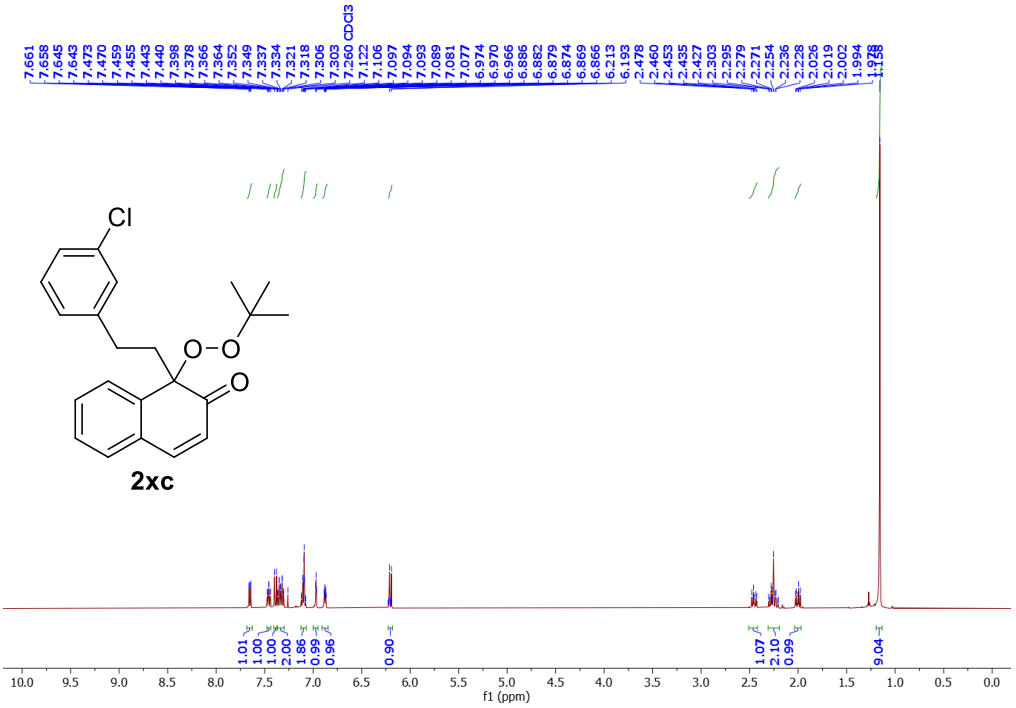

Figure 19. ^{1}H **NMR** of Compound **2xc**

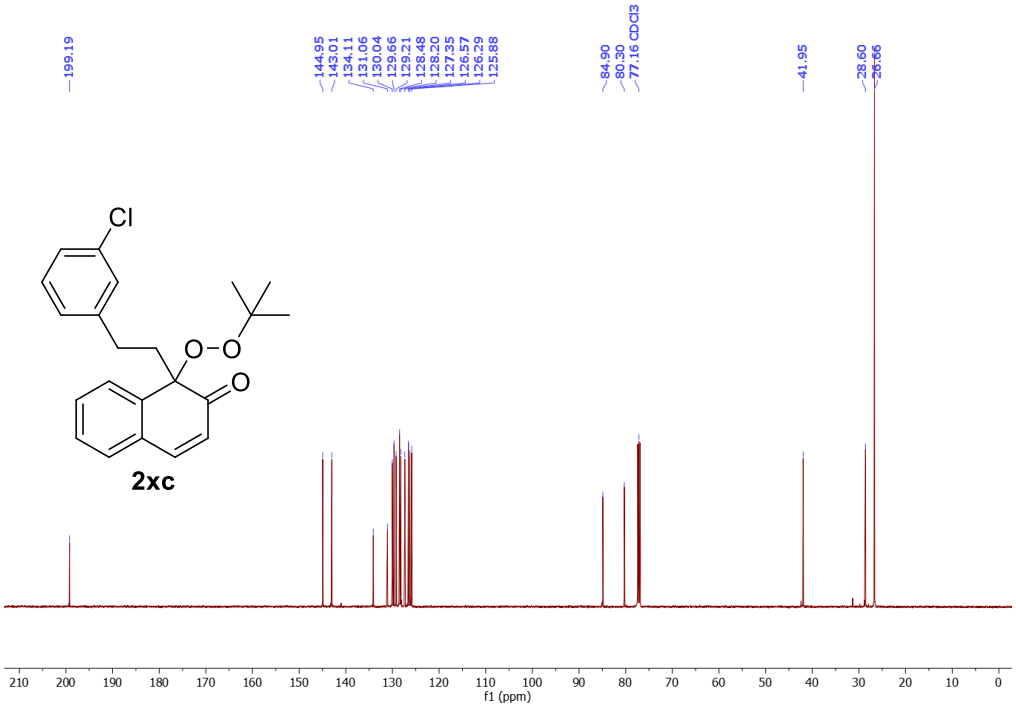

Figure 20. $^{13}C\{^{1}H\}$ **NMR** of Compound **2xc**

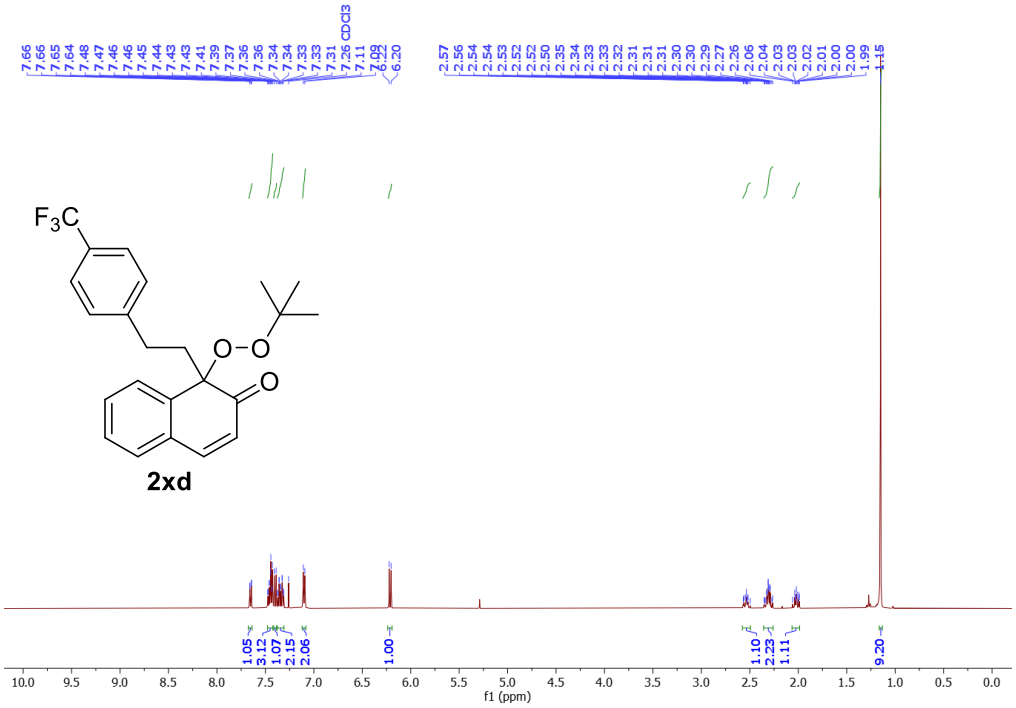

Figure 21. ^{1}H **NMR** of Compound **2xd**

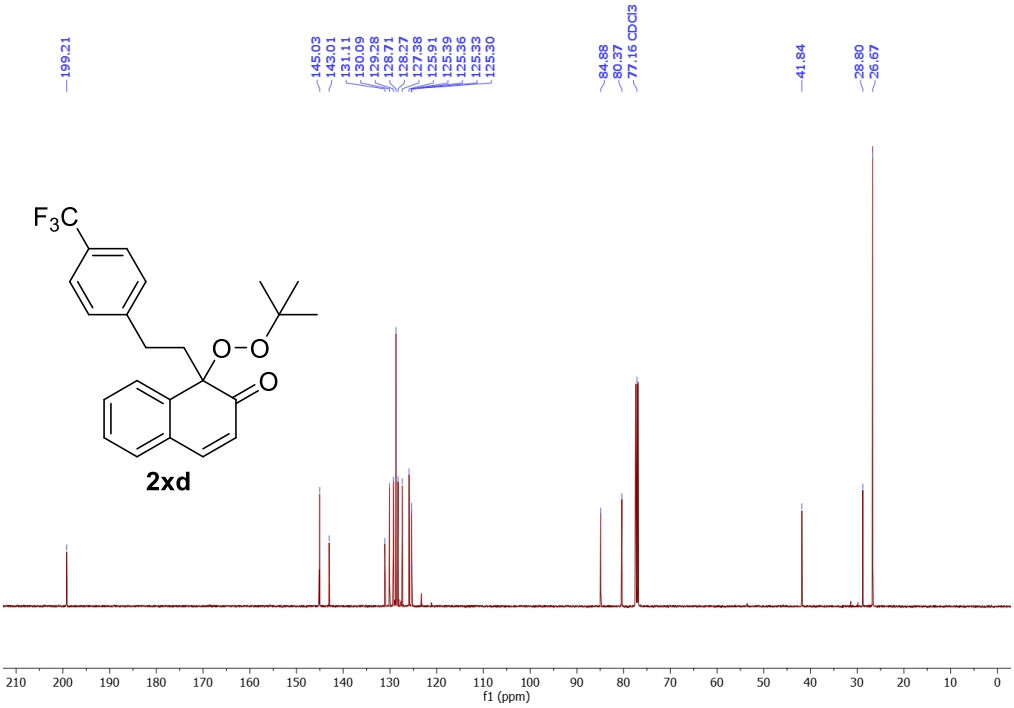

Figure 22. $^{13}C\{^{1}H\}$ **NMR** of Compound **2xd**

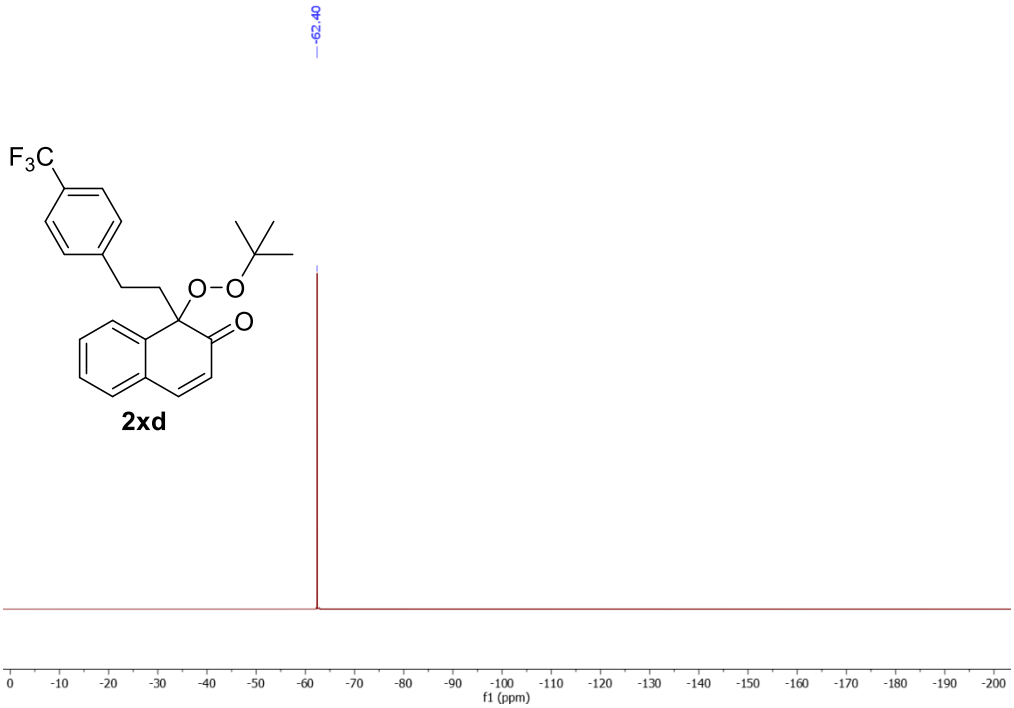

Figure 23. $^{19}F\{^{1}H\}$ **NMR** of Compound **2xd**

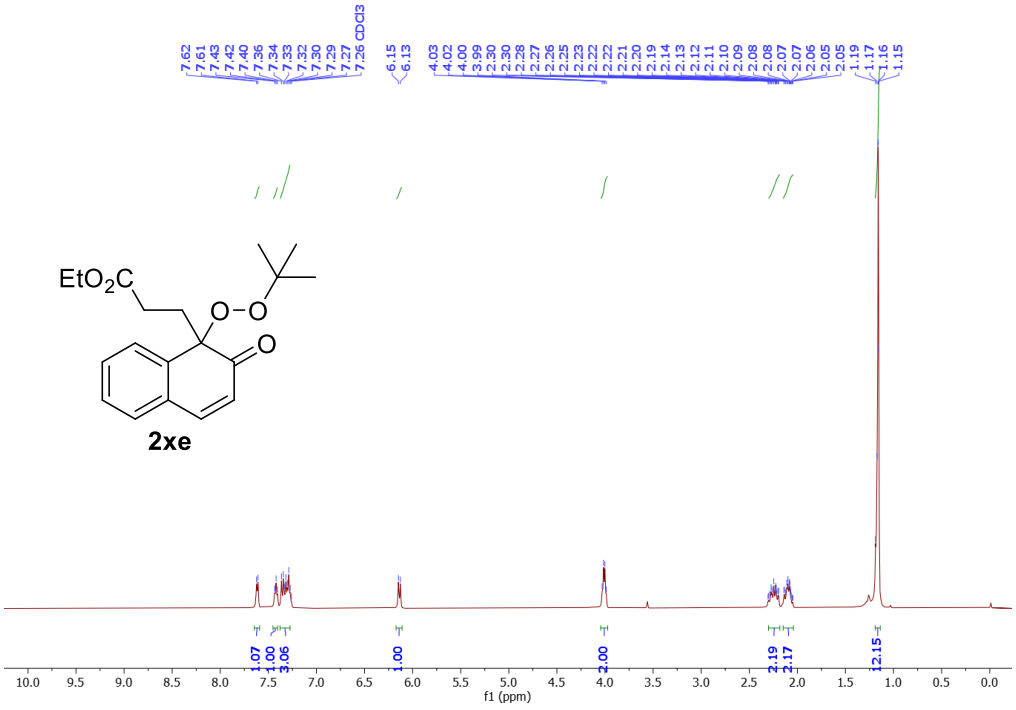

Figure 24. **^{1}H NMR** of Compound **3xe**

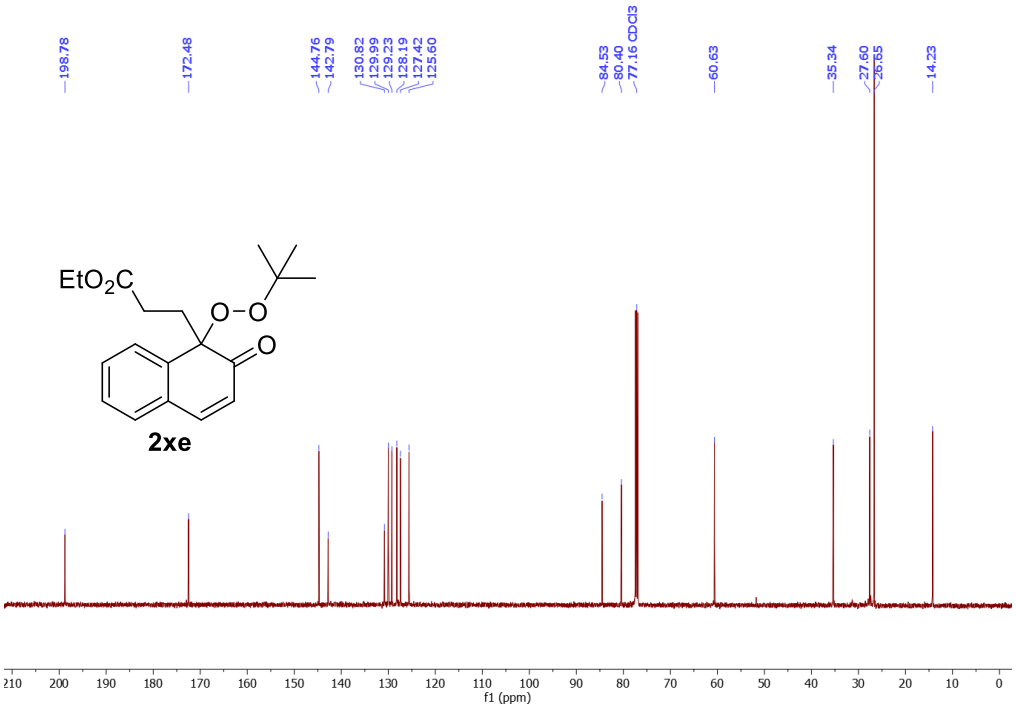

Figure 25. **^{13}C{^{1}H} NMR** of Compound **2xe**

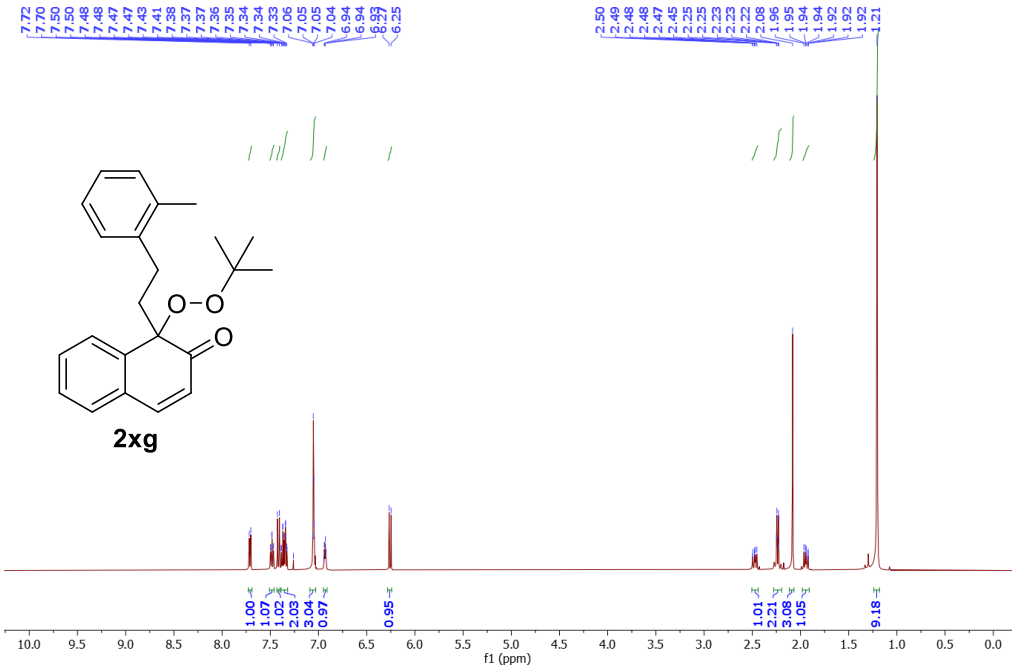

Figure 26. **^{1}H NMR** of Compound **2xg**

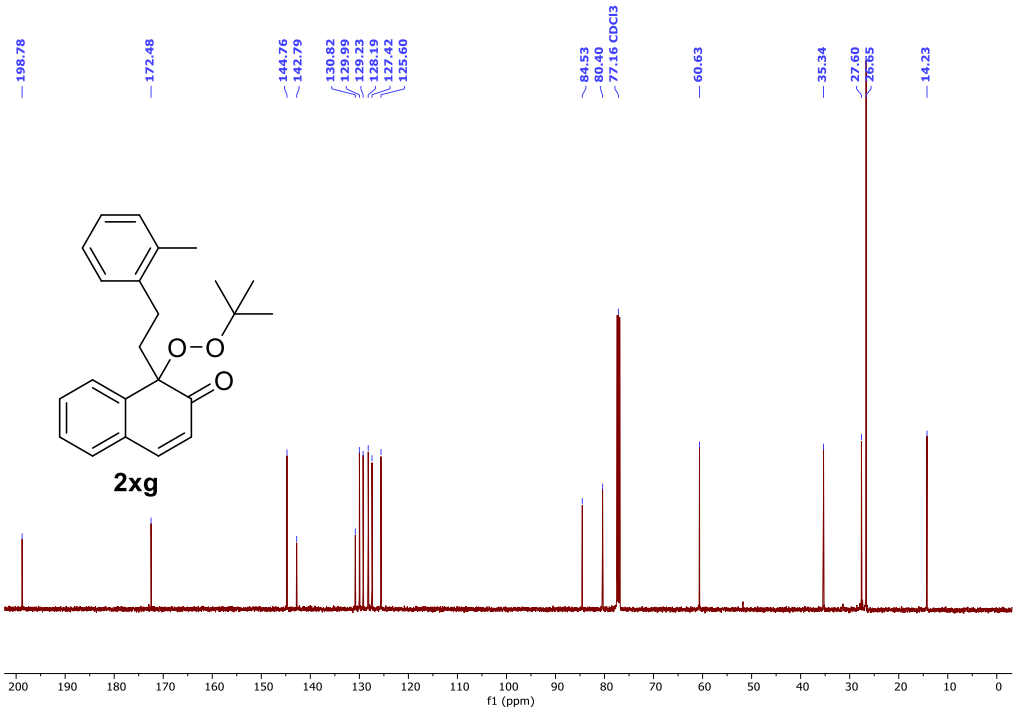

Figure 27. **^{13}C{^{1}H} NMR** of Compound **2xg**

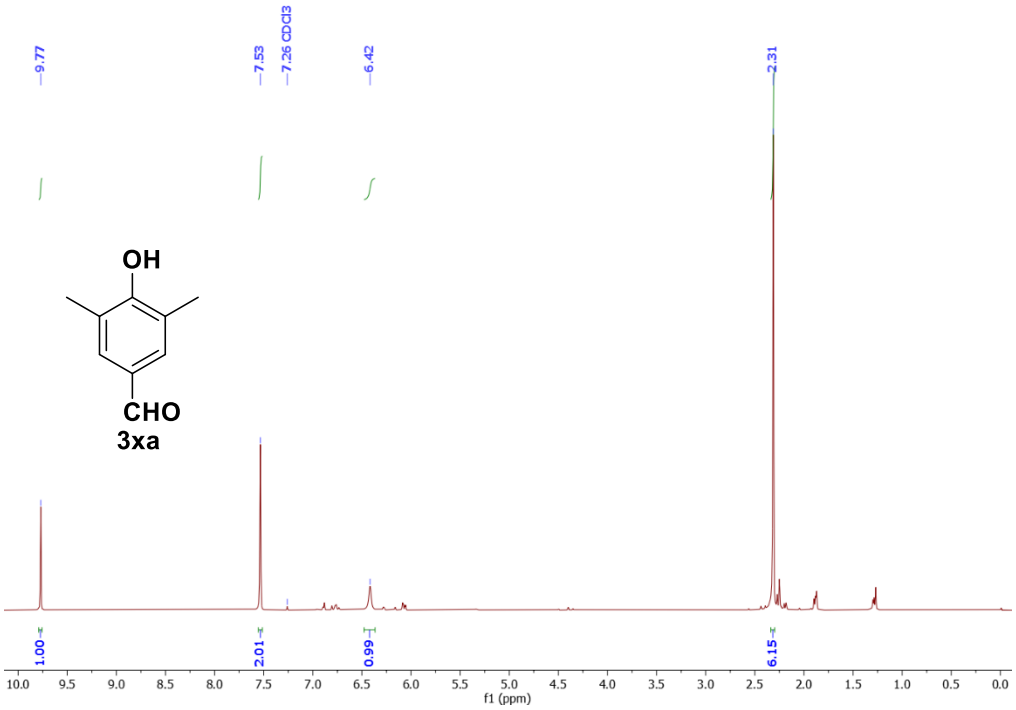

Figure 28. **^{1}H NMR** of Compound **3xa**

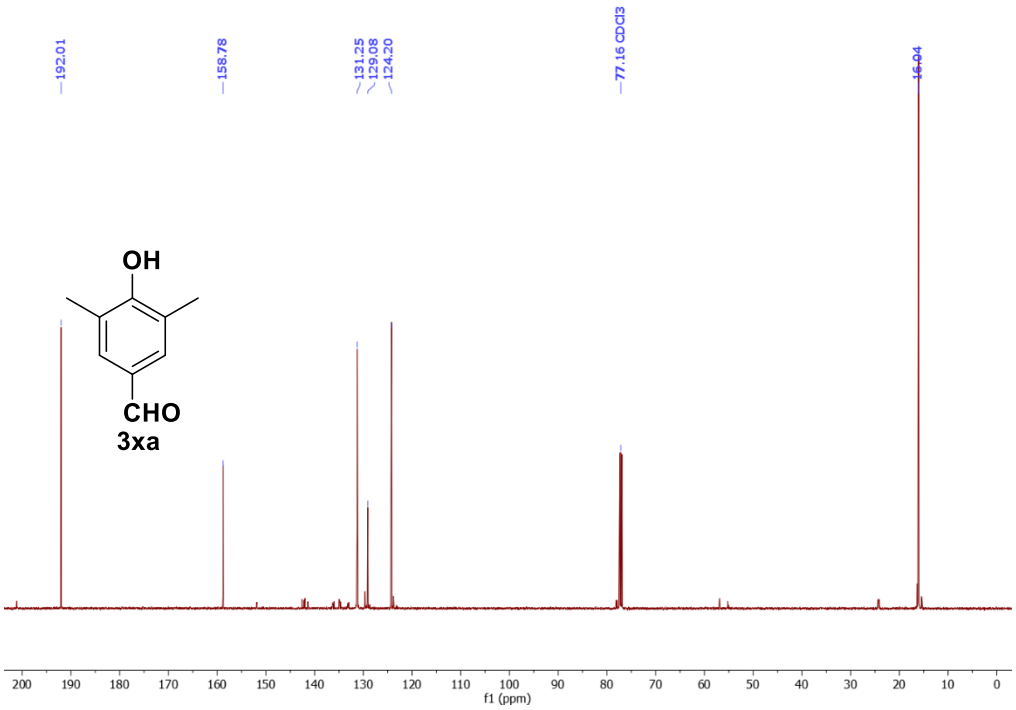

Figure 29. **^{13}C{^{1}H} NMR** of Compound **3xa**

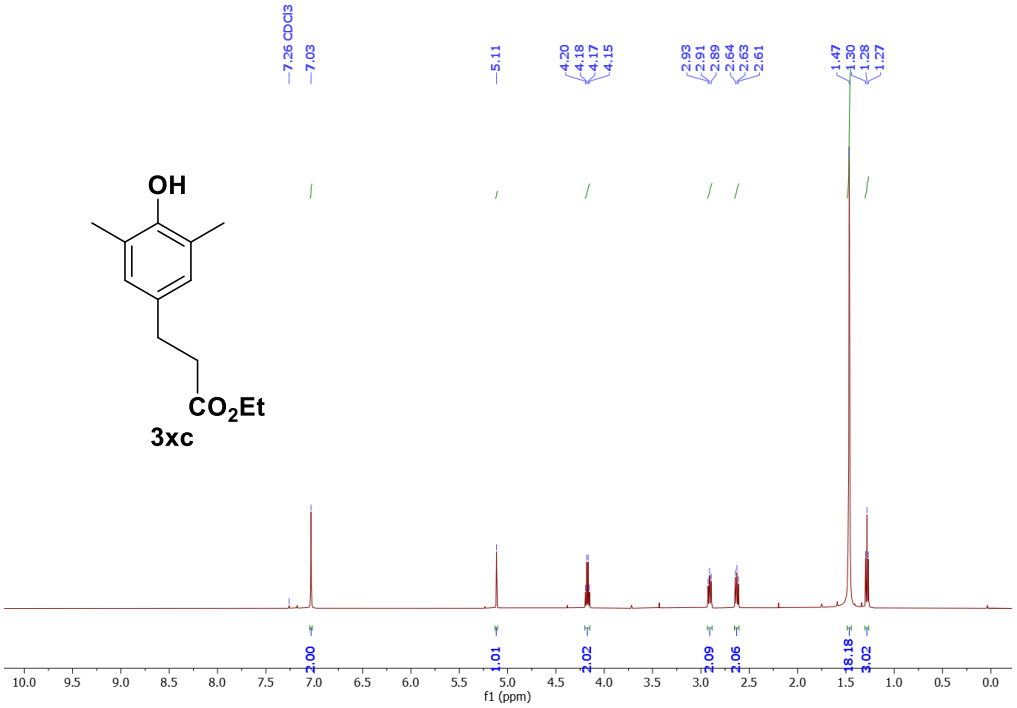

Figure 30. **^{1}H NMR** of Compound **3xc**

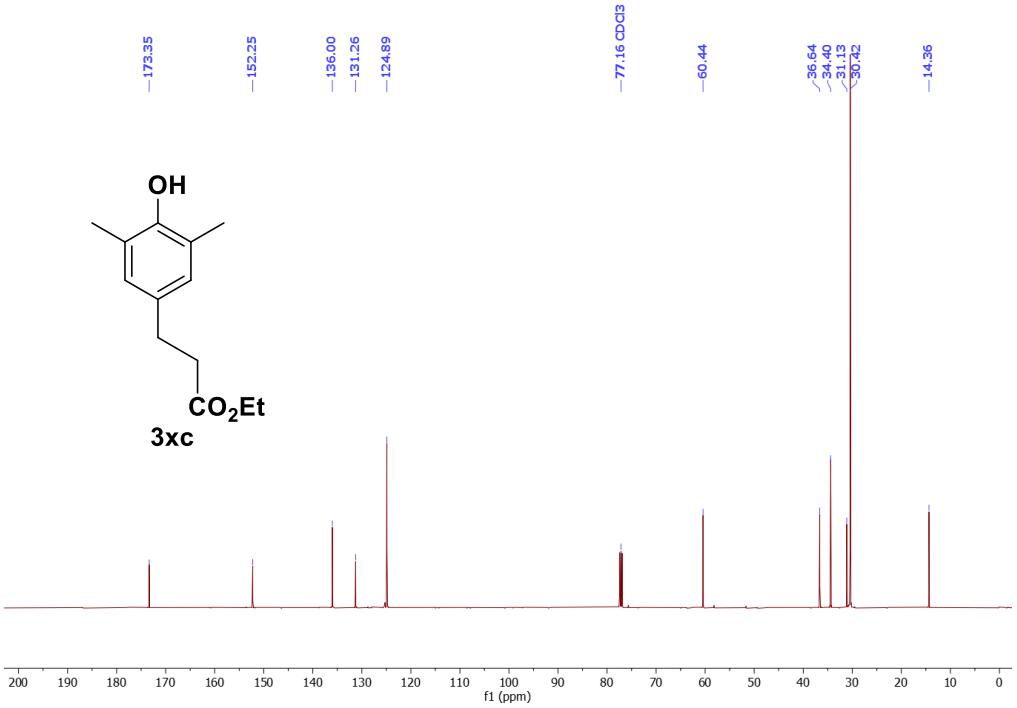

Figure 31. **^{13}C{^{1}H} NMR** of Compound **3xc**

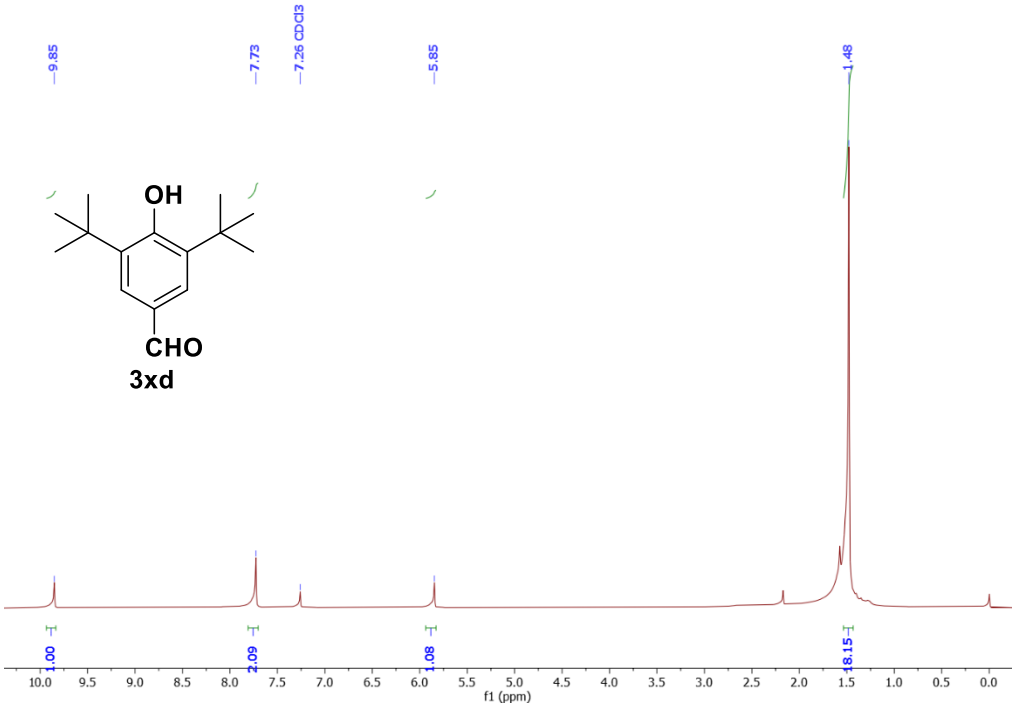

Figure 32. **^{1}H NMR** of Compound **3xd**

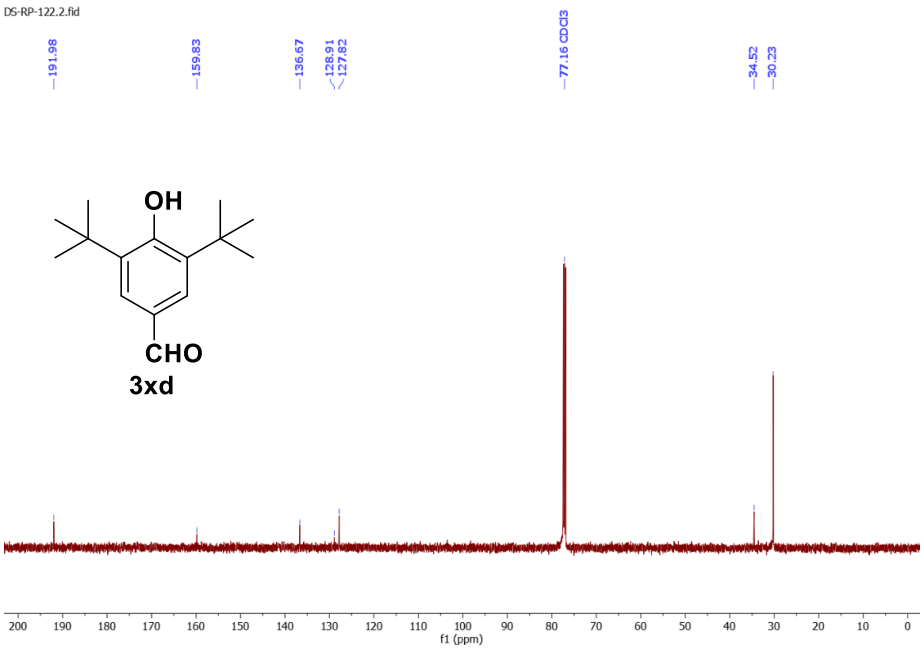

Figure 33. **^{13}C{^{1}H} NMR** of Compound **3xd**

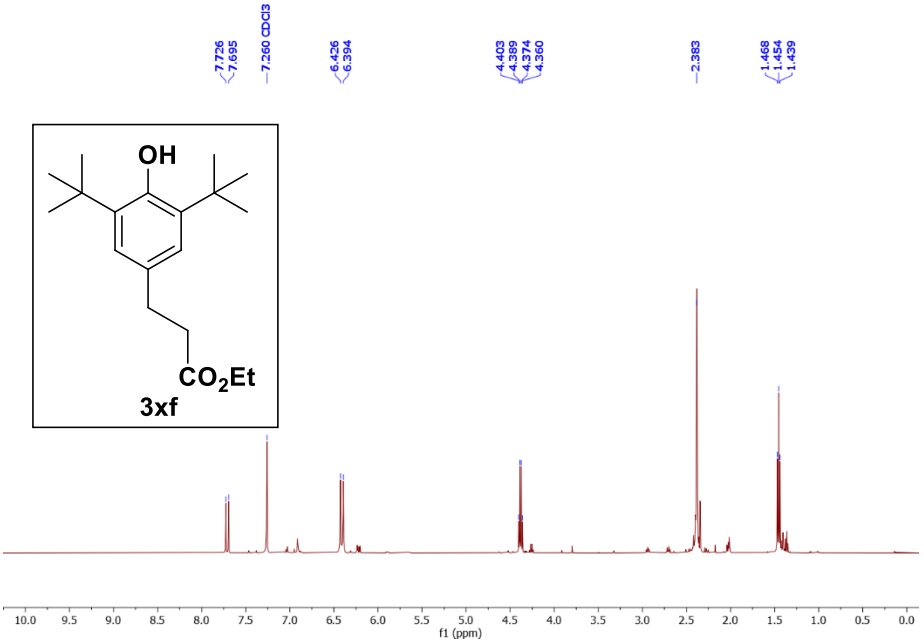

Figure 34. **^{1}H NMR** of Compound **3xf**

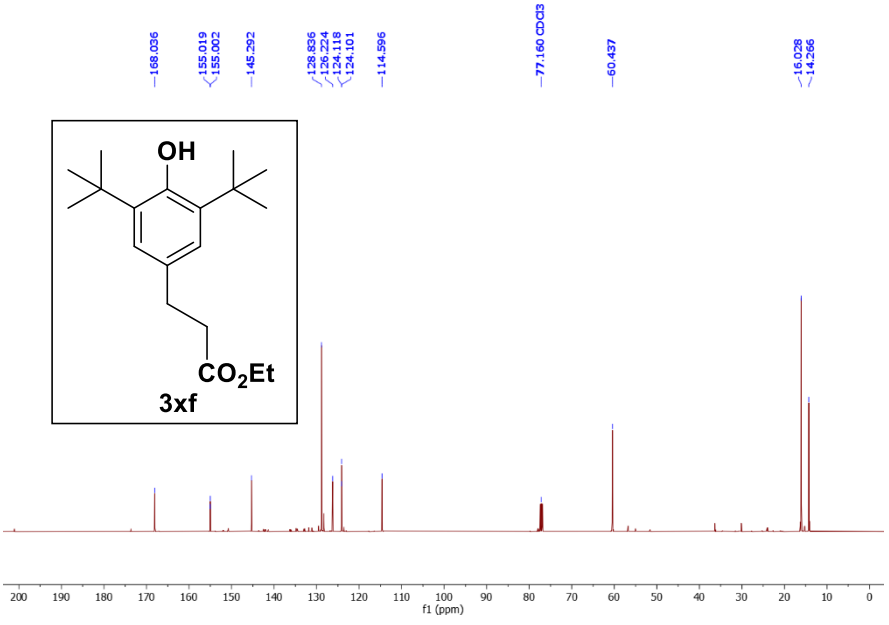

Figure 35. **^{13}C{^{1}H} NMR** of Compound **3xf**

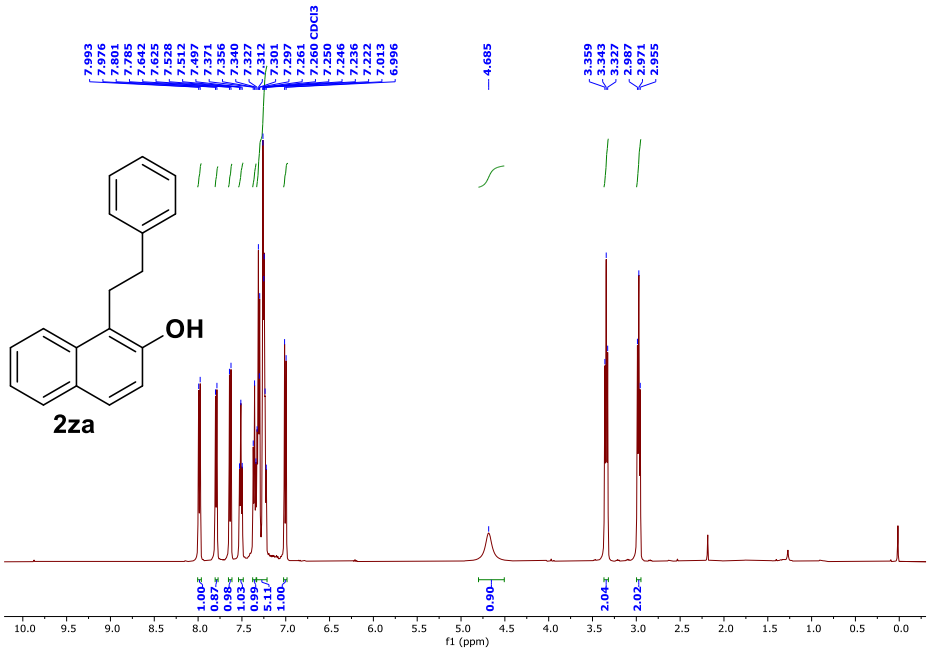

Figure 36. **^{1}H NMR** of compound **2za**

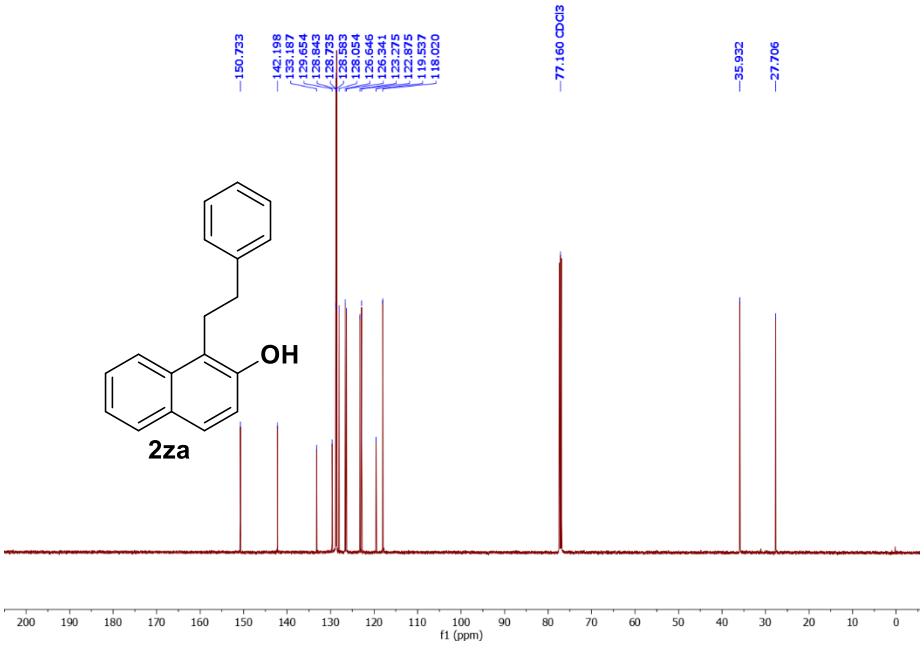

Figure 37. **^{13}C{^{1}H} NMR** of Compound **2za**

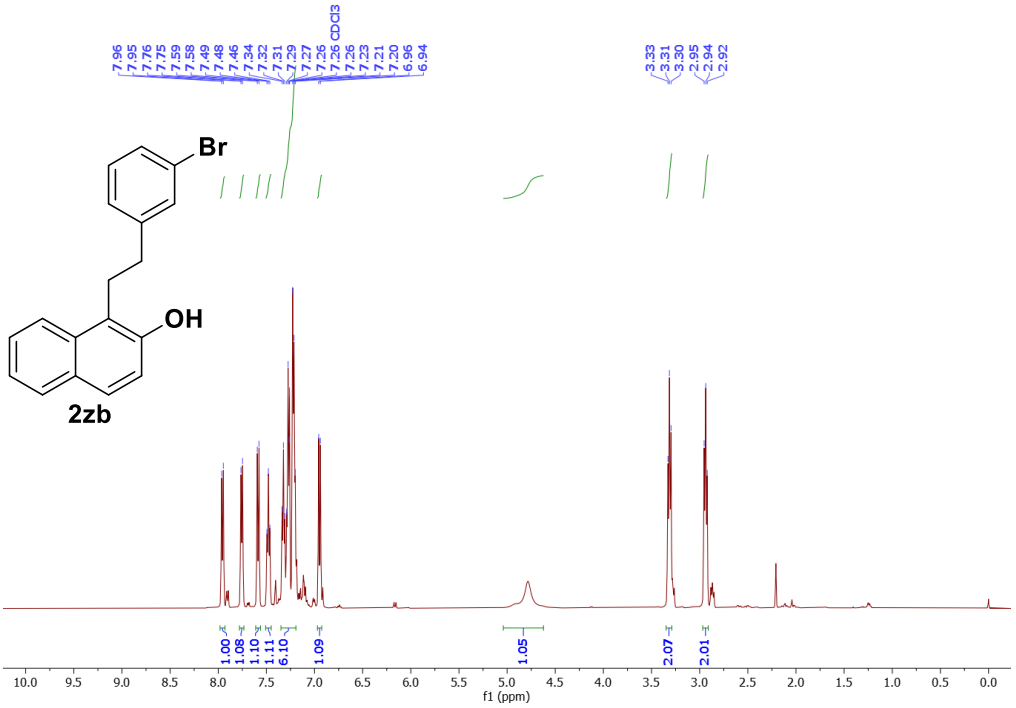

Figure 38. **^{1}H NMR** of Compound **2zb**

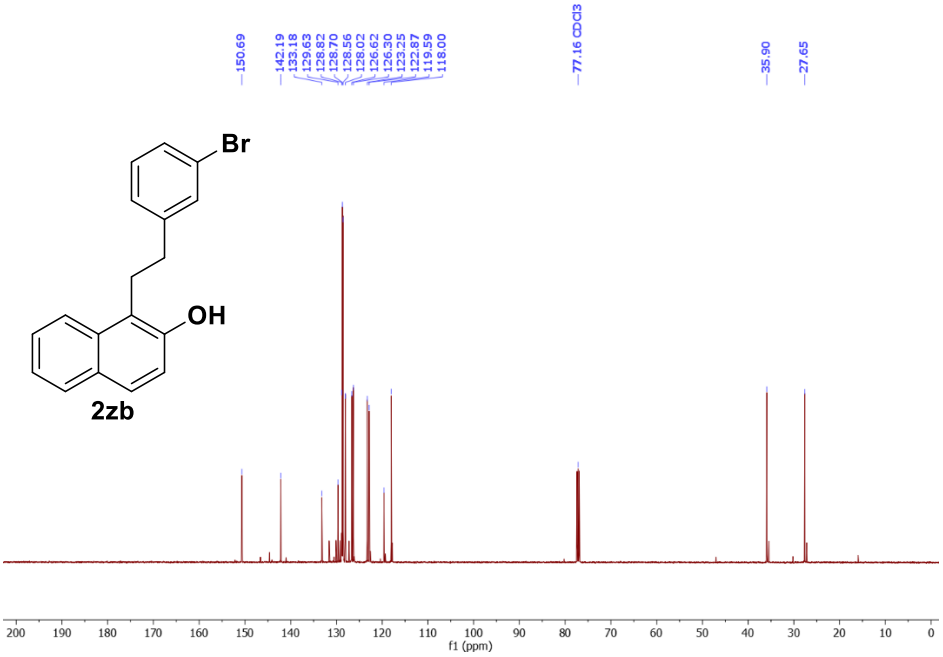

Figure 39. **^{13}C{^{1}H} NMR** of Compound **2zb**

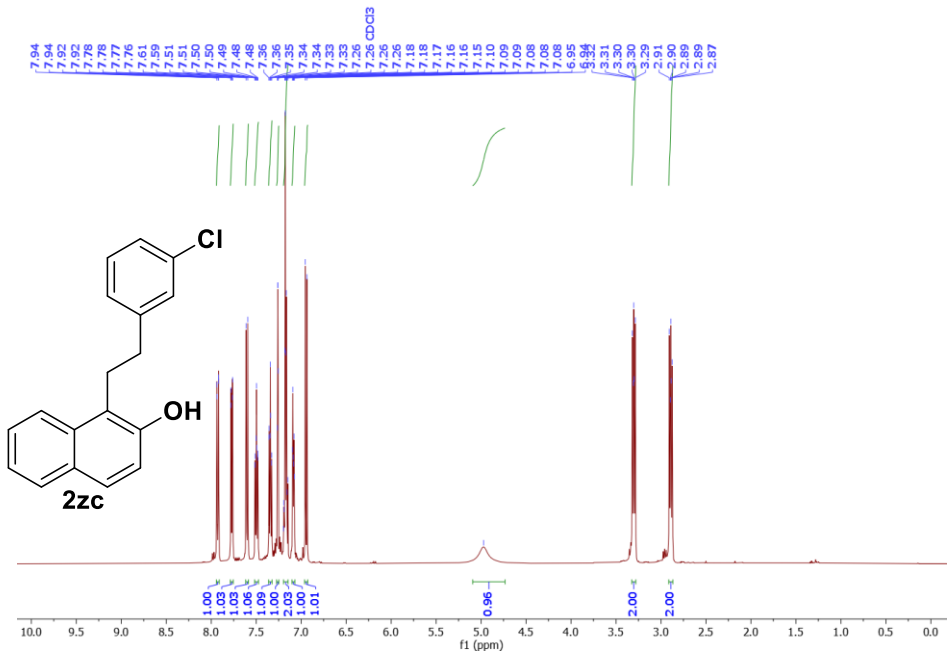

Figure 40. **^{1}H NMR** of Compound **2zc**

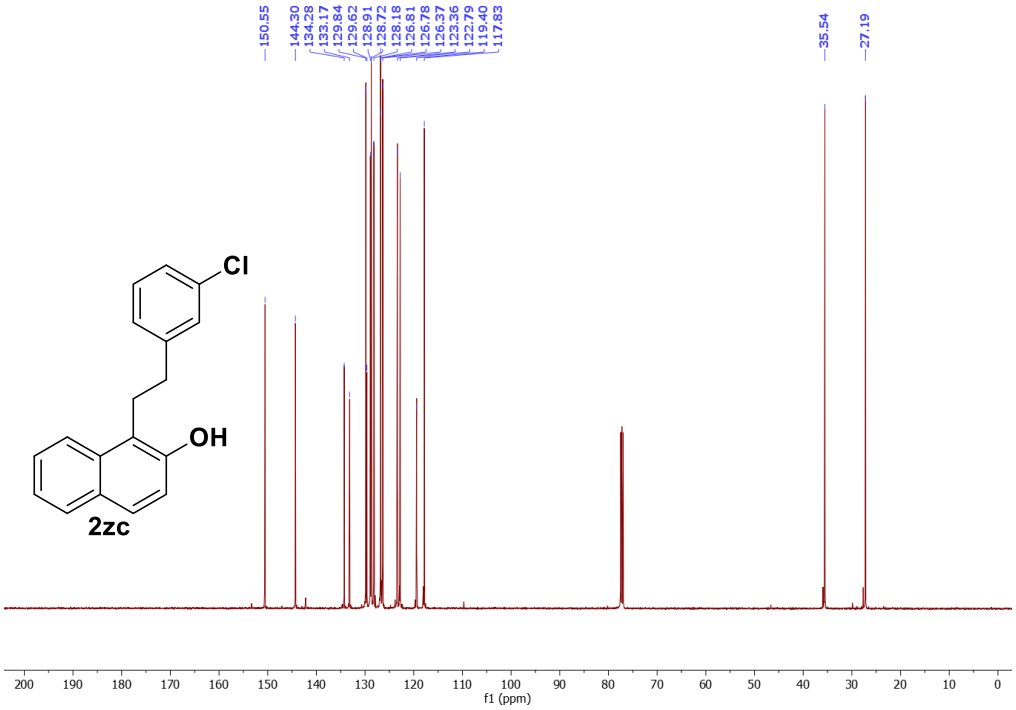

Figure 41. **^{13}C{^{1}H} NMR** of Compound **2zc**

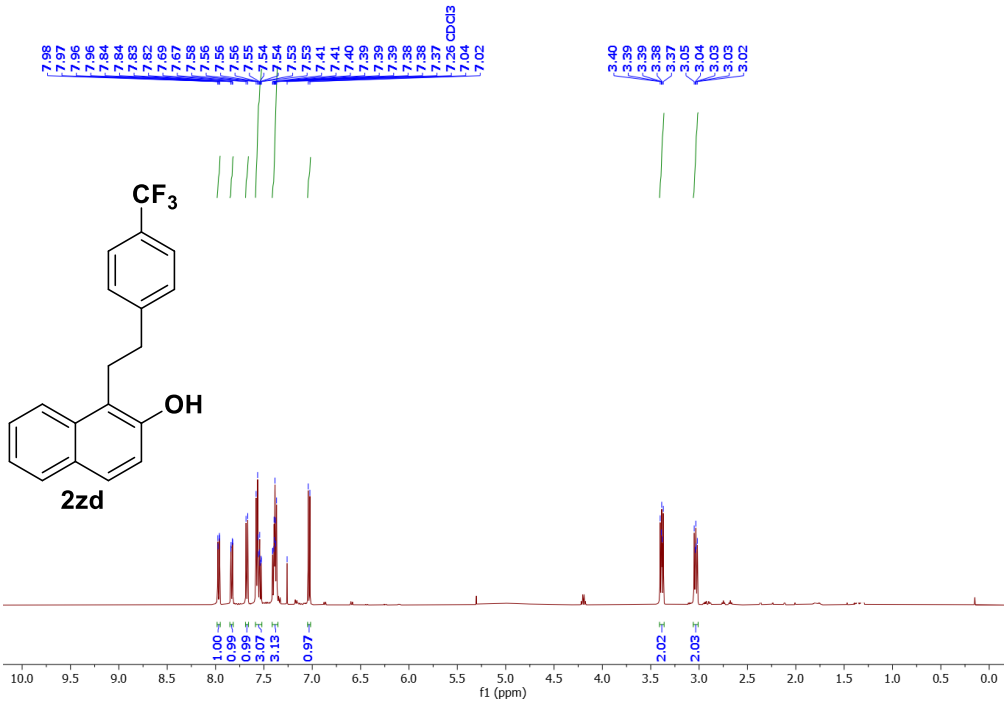

Figure 42. **^{1}H NMR** of Compound **2zd**

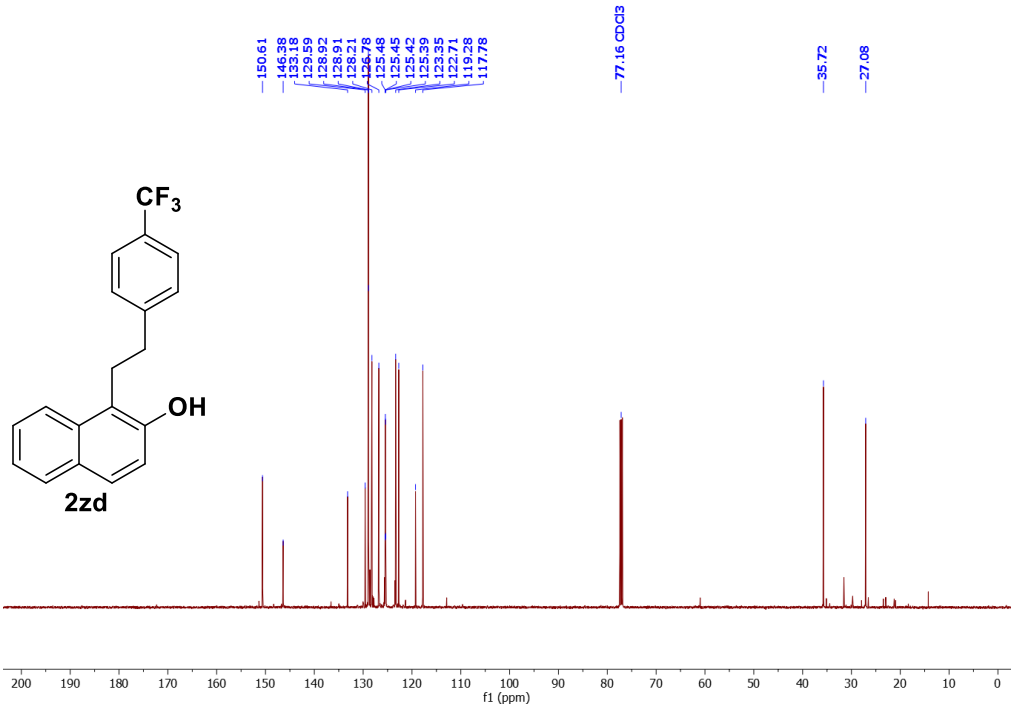

Figure 43. **^{13}C{^{1}H} NMR** of Compound **2zd**

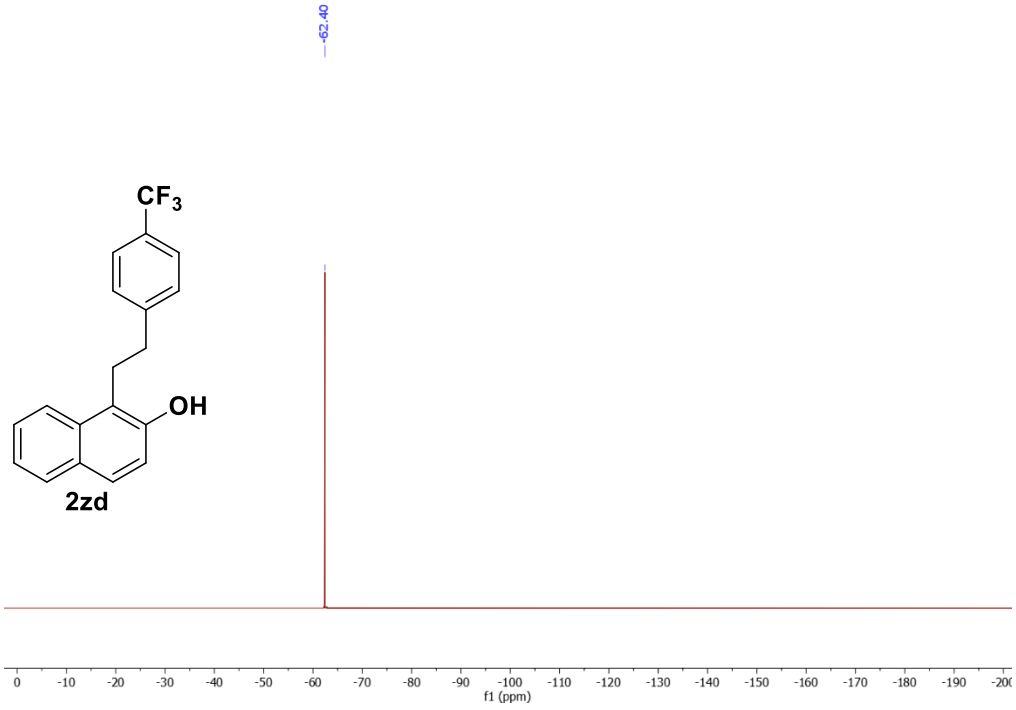

Figure 44. $^{19}F\{^{1}H\}$ **NMR** of Compound **2zd**

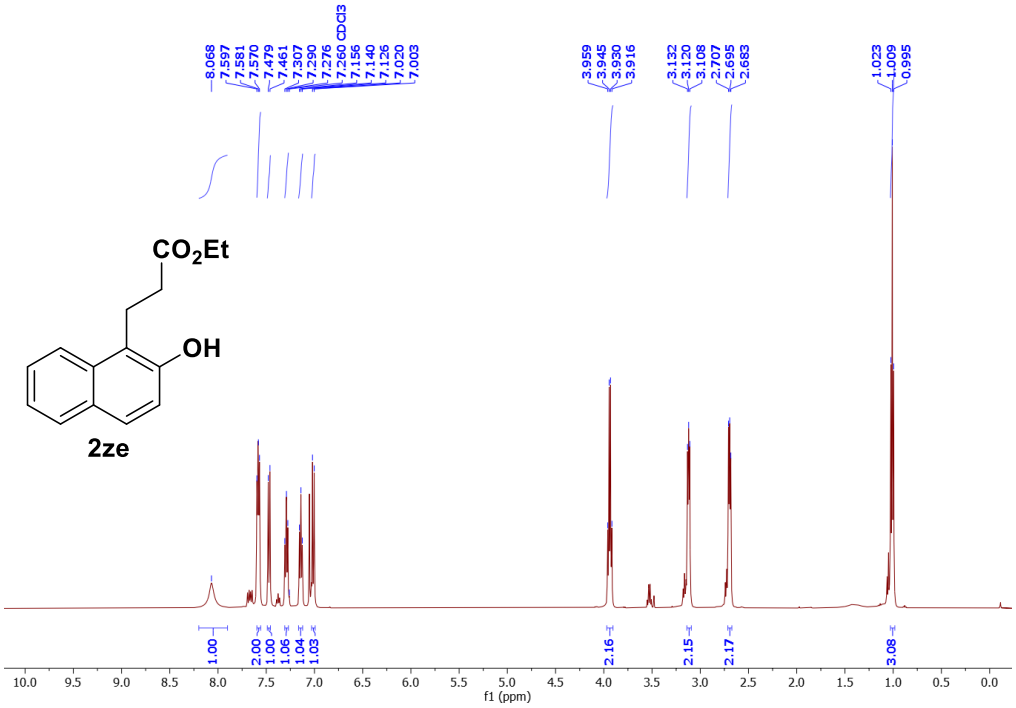

Figure 45. ^{1}H **NMR** of Compound **2ze**

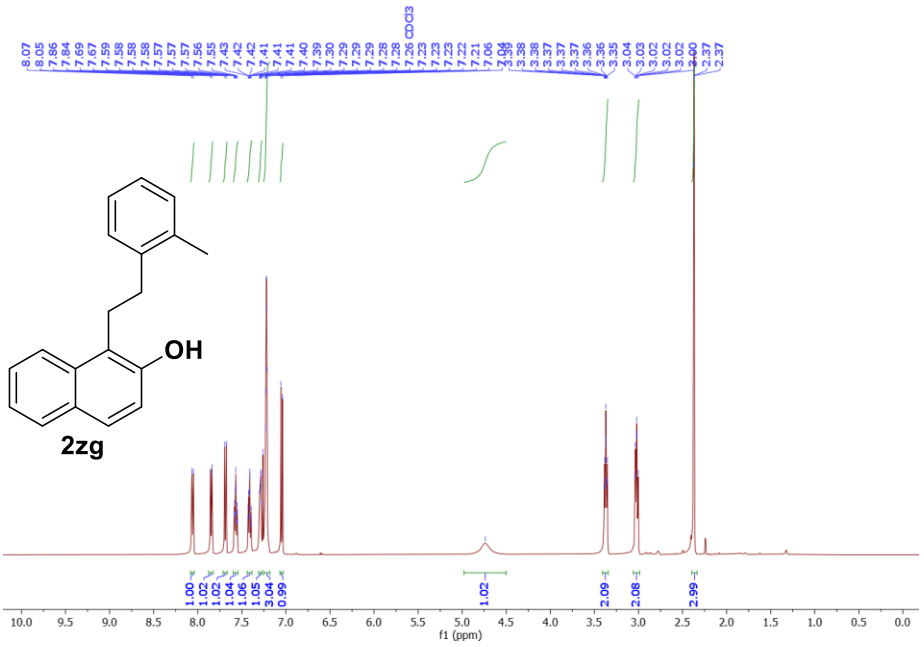

Figure 46. **^{1}H NMR** of Compound **2zg**

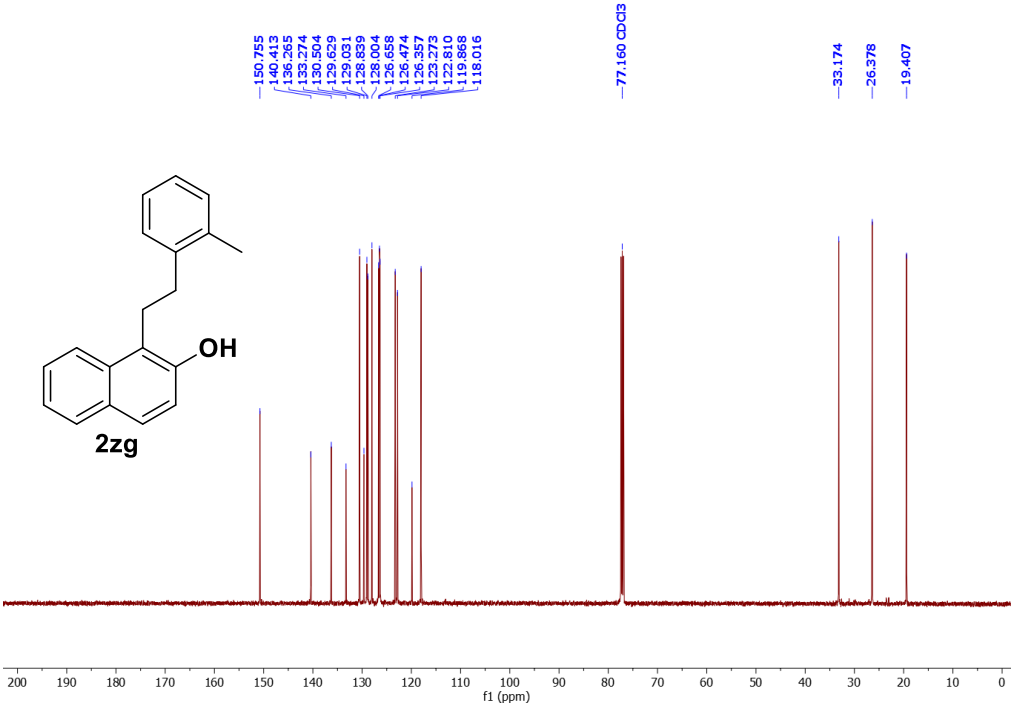

Figure 47. **^{13}C{^{1}H} NMR** of Compound **2zg**

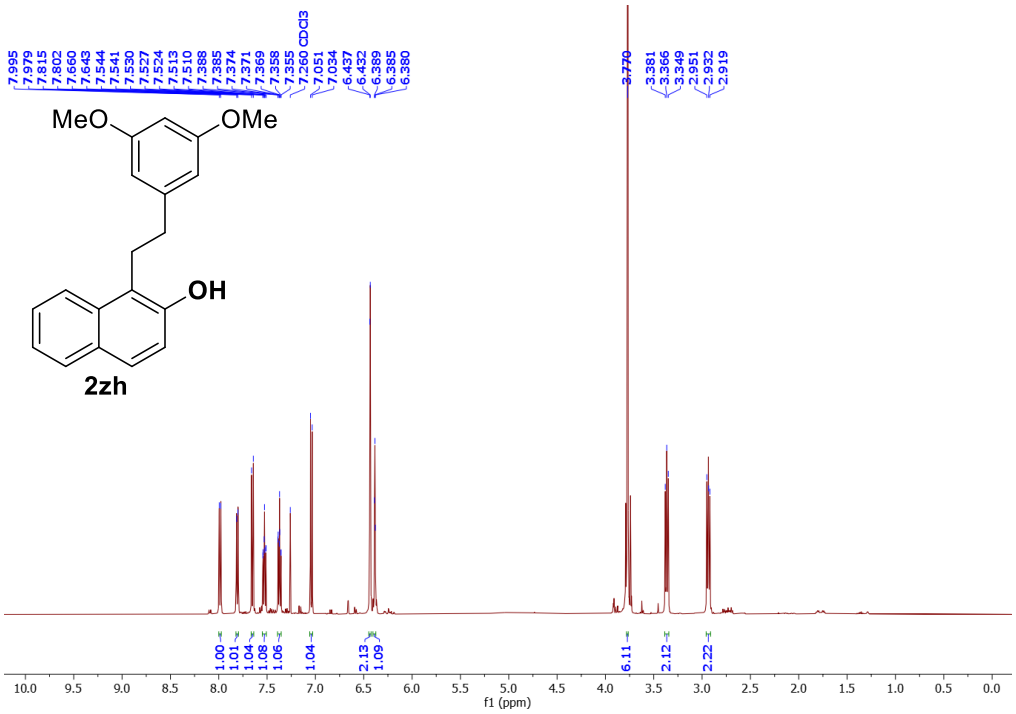

Figure 48. ***^{1}H NMR*** *of Compound* ***2zh***

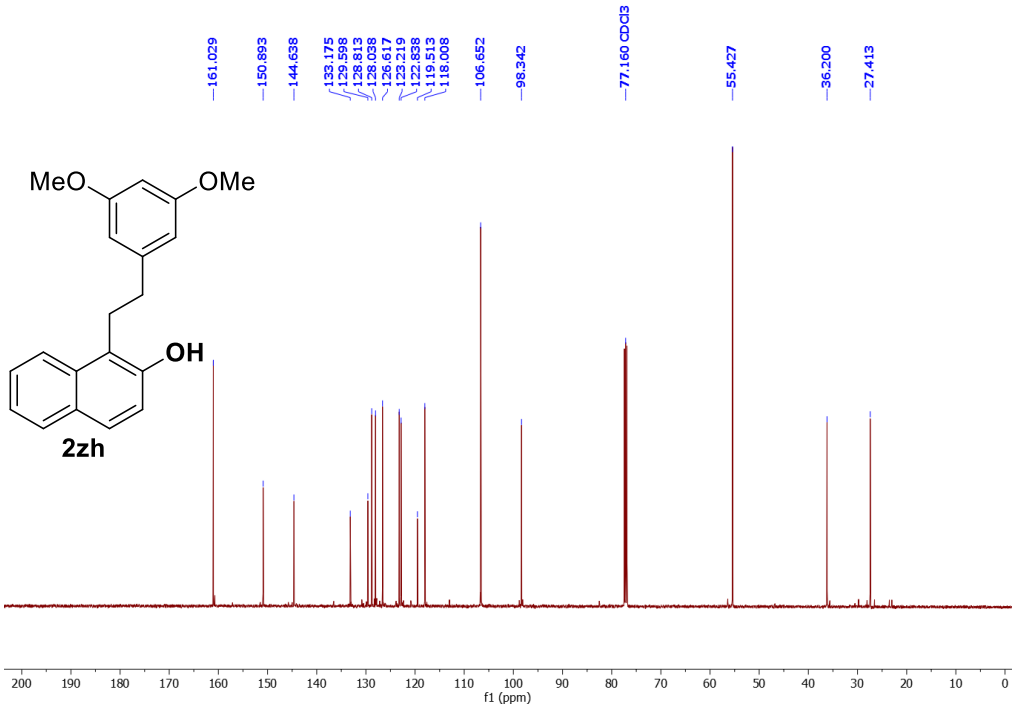

Figure 49. **^{13}C{^{1}H} NMR** of Compound **2zh**

Conclusions:

Here, we have successfully Synthesized a wide range of substituted phenols and naphthols and dearomatized them using a catalytic approach to bring the molecular complexity. The protocol works in mild conditions, room temperature, visible light for activation, and metal free. All the compounds are characterized by ^{1}H and $1^{3}C$ NMR.

Future Work:

We will increase the substrate scope. We will try to do enantioselectivity dearomatization by using chiral ammonium or phosphorous bromide and their functionalization will be carried out with their synthetic diversification. A variety of peroxides will be applied along with Thiols.

References:

1. Moriarty, R.M. and Prakash, O., 1986. Hypervalent iodine in organic synthesis. *Accounts of Chemical Research*, *19*(8), pp.244-250.
2. Zhuo, C.X., Zhang, W. and You, S.L., 2012. Catalytic asymmetric dearomatization reactions. *Angewandte Chemie International Edition*, *51*(51), pp.12662-12686.
3. Dabestani, R., Wang, X., Bard, A.J., Campion, A., Fox, M.A., Webber, S.E. and White, J.M., 1986. Photoinduced oxidation of bromide to bromine on irradiated platinized titanium dioxide powders and platinized titanium dioxide particles supported on Nafion films. *The Journal of Physical Chemistry*, *90*(12), pp.2729-2732.
4. Reichman, B. and Byvik, C.E., 1981. Photoproduction of I2, Br2, and Cl2 on n-semiconducting powder. *The Journal of Physical Chemistry*, *85*(15), pp.2255-2258.
5. Maniatakou, A., Parsons, S. and Karaliota, A., 2007. Photosensitized oxidation of bromide to bromine catalyzed by niobium pentachloride in methanol solution: Formation and crystal structure of the tetraphenylphosphonium

tribromide. *Journal of Photochemistry and Photobiology A: Chemistry*, *192*(1), pp.29-35.

6. Sarkar, D., Ghosh, M.K., Rout, N. and Kuila, P., 2017. "A Jack of Trio"-robust one-pot metal free oxidative amination, azidation and peroxidation of phenols. *New Journal of Chemistry*, *41*(10), pp.3715-3718.
7. Sarkar, D., Ghosh, M.K. and Rout, N., 2016. Phenyl trimethyl ammonium tribromide mediated robust one-pot synthesis of spiro-oxacycles–an economic route–stereoselective synthesis of oxaspirohexacyclodieneones. *Organic & Biomolecular Chemistry*, *14*(33), pp.7883-7898.
8. Roy, B., Kuila, P. and Sarkar, D., 2024. Visible-light Catalysed Trifluoromethylthiolation and Related Dearomative Spirocyclizations. *Advanced Synthesis & Catalysis*.
9. Das, B., Sahoo, S.R., Das, A., Pathak, B. and Sarkar, D., 2023. Sustainable Organic Photocatalysis for Site-Selective Hydrazocoupling of Electron-Rich Arenes. *Organic Letters*, *25*(42), pp.7733-7738.
10. Sarkar, D. and Rout, N., 2019. Ruthenium (VIII)-catalyzed ipso-dearomative spiro-etherification and spiro-amidation of phenols. *Organic letters*, *21*(11), pp.4132-4136.
11. Baker Dockrey, S.A., Lukowski, A.L., Becker, M.R. and Narayan, A.R., 2018. Biocatalytic site-and enantioselective oxidative dearomatization of phenols. *Nature chemistry*, *10*(2), pp.119-125.